SAND2022-12706C

3D SIMULATIONS CAPTURE THE PERSISTENT LOW MODE ASYMMETRIES EVIDENT IN LASER-DIRECT-DRIVE IMPLOSIONS ON OMEGA

ECLIM 2022

SEPT 21ST, 2022

A. COLAITIS[1], I. IGUMENSCHEV[2], D. TURNBULL[2], R. SHAH[2], D. EDGELL[2], O. MANNION[3], R. FOLLETT[2], D. STROZZI[4], T. CHAPMAN[4], C. STOECKL[2], D. JACOB-PERKINS[2], A. SHVYDKY[2], R. JANEZIC[2], A. KALB[2], D. CAO[2], C. J. FORREST[2], J. KWIATKOWSKI[2], S. REGAN[2], W. THEOBALD[2], V. GONCHAROV[2], D. FROULA[2]

1. CELIA, BORDEAUX
2. LLE, ROCHESTER NY
3. SANDIA NATIONAL LABORATORIES*, NM
4. LLNL, LIVERMORE CA

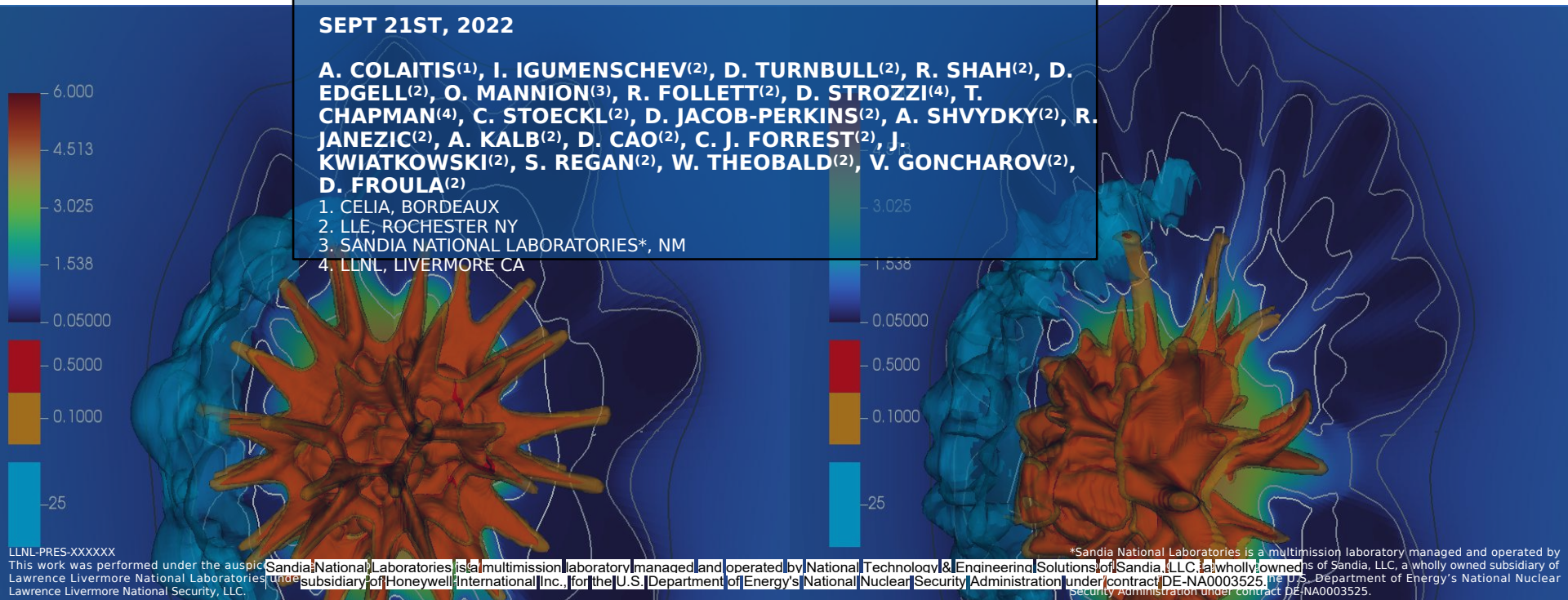

LLNL-PRES-XXXXXX
This work was performed under the auspic Lawrence Livermore National Laboratories Lawrence Livermore National Security, LLC.

Sandia National Laboratories is a multimission laboratory managed and operated by National Technology & Engineering Solutions of Sandia, LLC, a wholly owned subsidiary of Honeywell International Inc., for the U.S. Department of Energy's National Nuclear Security Administration under contract DE-NA0003525.

*Sandia National Laboratories is a multimission laboratory managed and operated by ns of Sandia, LLC, a wholly owned subsidiary of he U.S. Department of Energy's National Nuclear Security Administration under contract DE-NA0003525.

DIRECT-DRIVE ICF RELIES ON HIGH LEVELS OF SYMMETRY TO REACH HIGH GAINS, WHICH ARE NECESSARY FOR ENERGY PRODUCTION

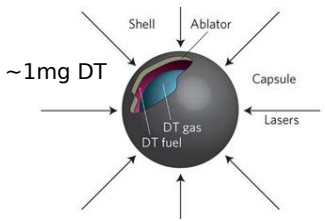

heating

implosion

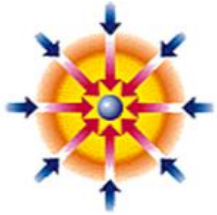

ignition

burn

DIRECT-DRIVE ICF RELIES ON HIGH LEVELS OF SYMMETRY TO REACH HIGH GAINS, WHICH ARE NECESSARY FOR ENERGY PRODUCTION

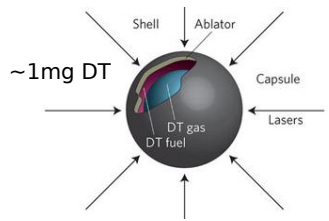

heating

implosion

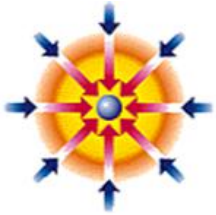

ignition

burn

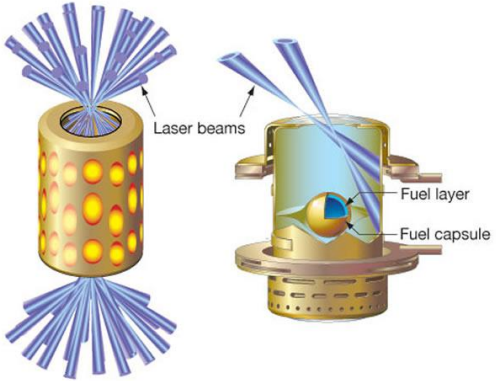

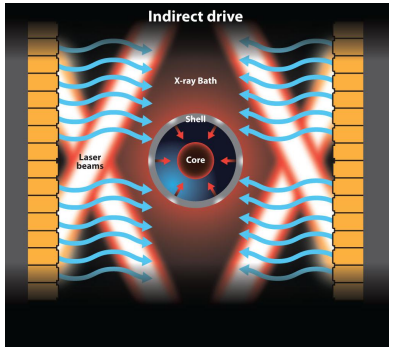

Indirect-drive approach

- Lower gain (X-ray conversion)
- Higher drive smoothness
- Time-dependant cylindrical drive to implode a spherical capsule

DIRECT-DRIVE ICF RELIES ON HIGH LEVELS OF SYMMETRY TO REACH HIGH GAINS, WHICH ARE NECESSARY FOR ENERGY PRODUCTION

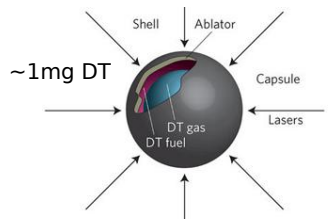

heating

implosion

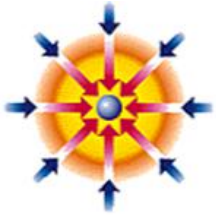

ignition

burn

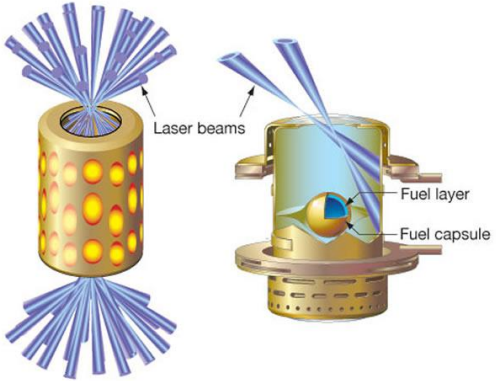

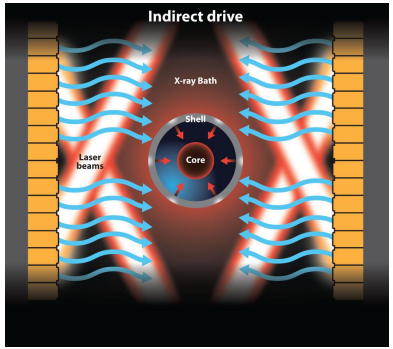

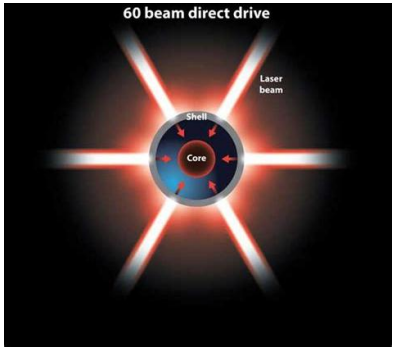

Indirect-drive approach

- Lower gain (X-ray conversion)
- Higher drive smoothness
- Time-dependant cylindrical drive to implode a spherical capsule

Direct-drive approach => favored for energy production

- Higher gain
- More sensitive to 3D laser effects (imbalance, alignment, etc) and beam smoothness

Understanding the sources of implosion perturbations is key to reach high gains for inertial fusion energy

BEST-SETUP EXPERIMENTS ON OMEGA IN 2019-2020 EXHIBIT SYSTEMATIC FLOW ANOMALIES

Database of 111 shots conducted in 2019-2020 on OMEGA
=> down-selection of 12 shots with:
- 60 beams, full SSD
- good ice thickness uniformity (<1% l=1)
- good ice surface roughness
- low pointing error (<2% l=1, <2% l=2 to <1% l =1)
- low power imbalance
- low target offset (< 5 microns to < 1 micron)

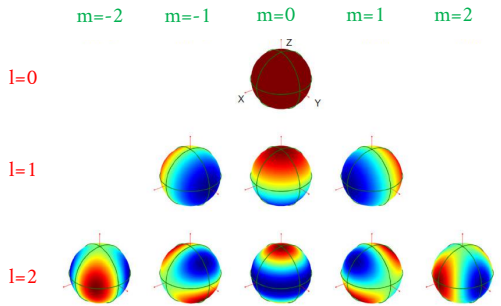

BEST-SETUP EXPERIMENTS ON OMEGA IN 2019-2020 EXHIBIT SYSTEMATIC FLOW ANOMALIES

Database of 111 shots conducted in 2019-2020 on OMEGA
=> down-selection of 12 shots with:
- 60 beams, full SSD
- good ice thickness uniformity (<1% l=1)
- good ice surface roughness
- low pointing error (<2% l=1, <2% l=2 to <1% l =1)
- low power imbalance
- low target offset (< 5 microns to < 1 micron)

... there remain a significant mode 1 assymetry in the DT flow at stagnation, that does not seem correlated to mispointing error, cryo/warm, or shot-day anomalies

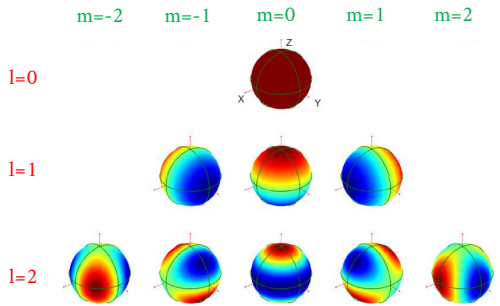

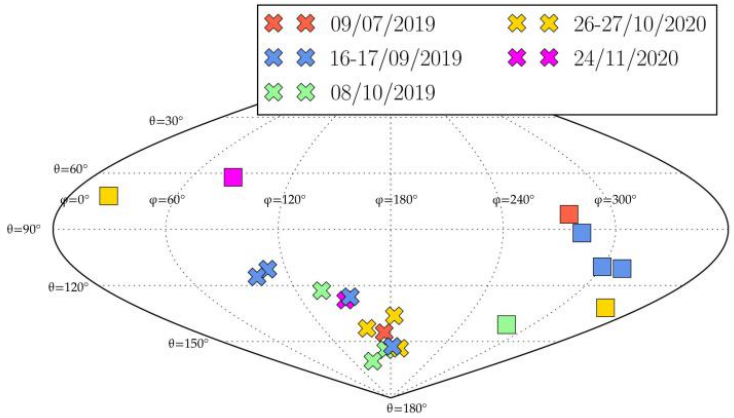

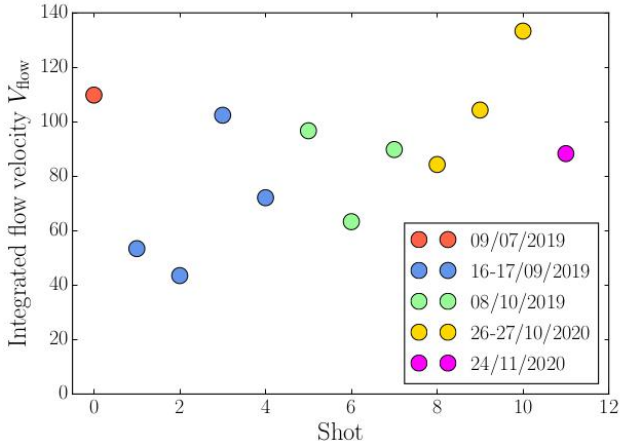

BEST-SETUP EXPERIMENTS ON OMEGA IN 2019-2020 EXHIBIT SYSTEMATIC FLOW ANOMALIES

Database of 111 shots conducted in 2019-2020 on OMEGA
=> down-selection of 12 shots with:
- 60 beams, full SSD
- good ice thickness uniformity (<1% l=1)
- good ice surface roughness
- low pointing error (<2% l=1, <2% l=2 to <1% l =1)
- low power imbalance
- low target offset (< 5 microns to < 1 micron)

... there remain a significant mode 1 assymetry in the DT flow at stagnation, that does not seem correlated to mispointing error, cryo/warm, or shot-day anomalies

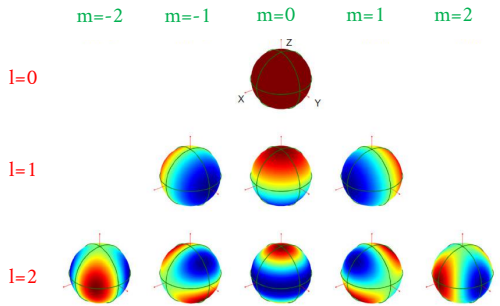

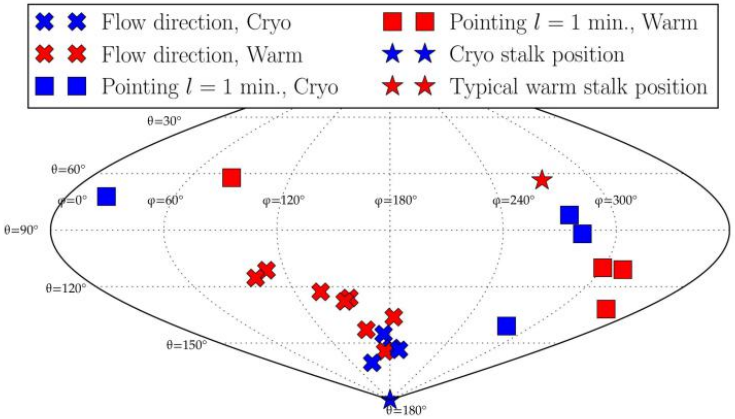

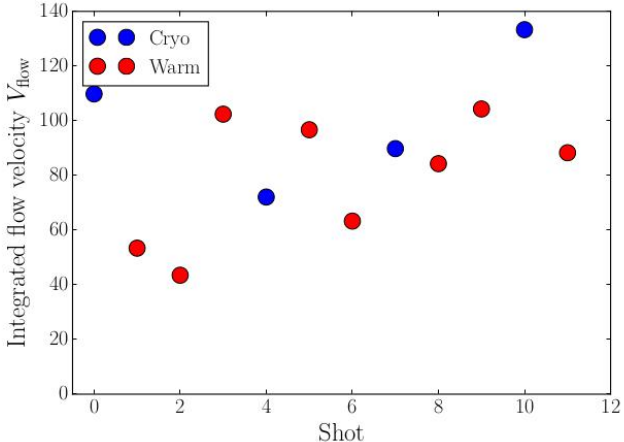

BEST-SETUP EXPERIMENTS ON OMEGA IN 2019-2020 EXHIBIT SYSTEMATIC FLOW ANOMALIES

Database of 111 shots conducted in 2019-2020 on OMEGA
=> down-selection of 12 shots with:
- 60 beams, full SSD
- good ice thickness uniformity (<1% l=1)
- good ice surface roughness
- low pointing error (<2% l=1, <2% l=2 to <1% l =1)
- low power imbalance
- low target offset (< 5 microns to < 1 micron)

... there remain a significant mode 1 assymetry in the DT flow at stagnation, that does not seem correlated to mispointing error, cryo/warm, or shot-day anomalies

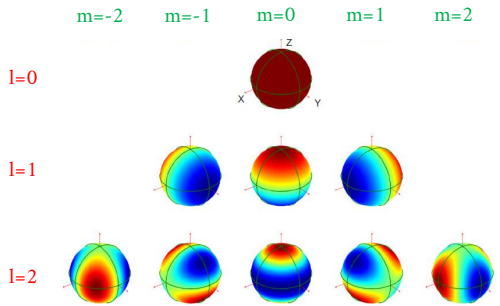

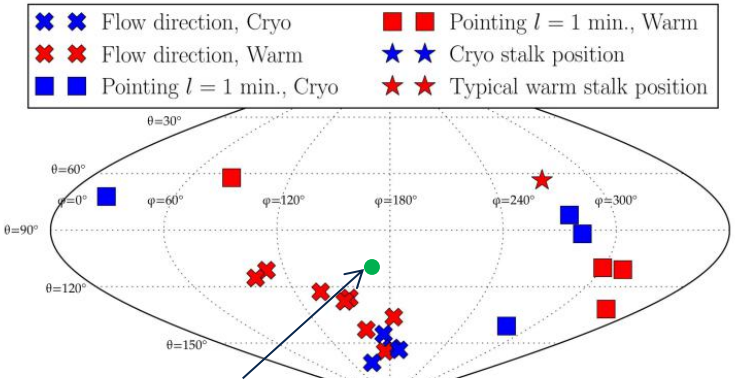

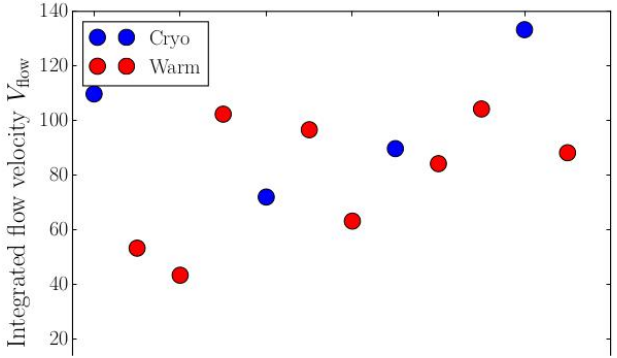

Low mode direction from offline calculation of CBET polarization effect [D. Edgell et al. PRL (2022)]

OUTLINE

- Is the polarization effect of CBET responsible for the systematic anomaly ?
- If including most sources of low modes, can the modeling reproduce the OMEGA measurements for neutron data ? (is the modeling also accurate for NIF direct-drive expts ?)
- What is the relative contribution of these sources to yield degradation ?
- How to mitigate low modes ?
- Early results from inline CBET with bandwidth: 1% bandwidth on OMEGA

UNPOLARIZED CBET FROM A SYMMETRIC BEAM PATTERN PRODUCES A SYMMETRIC IRRADIATION

Why would the polarization effect matter ... ?

Cross Beam Energy Transfer (CBET) transfers energy between beams through a shared IAW grating

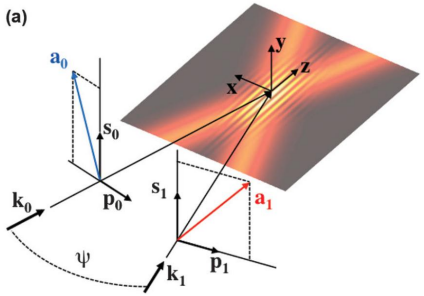

[P. Michel et al. PoP 17 (2010)]

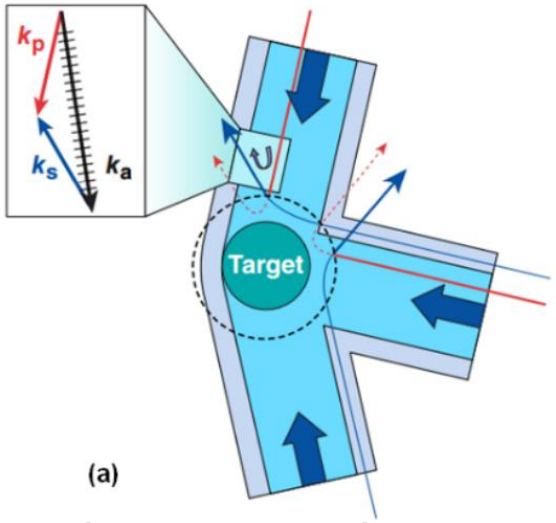

[A. K. Davis et al. PoP (2016)]

In direct-drive, reflected beams "steal" energy from incident beams

If the laser configuration is **perfectly symetric**, the unpolarized CBET also remains symmetric

POLARIZATION EFFECTS CONTRIBUTE TO THE DETAILS OF CBET AMPLIFICATION

Why would the polarization effect matter ... ?

- Ellipticity induced from propagation in a bi-refringent medium formed by the IAW grating
- Probe beam polarization rotation toward that of the pump
- Polarization transport through refraction

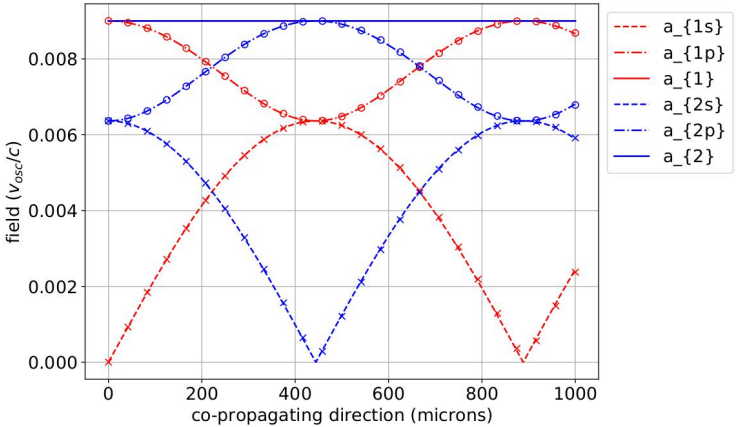

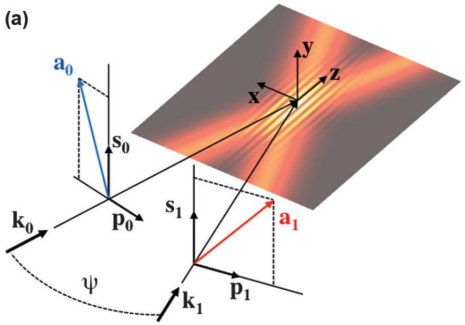

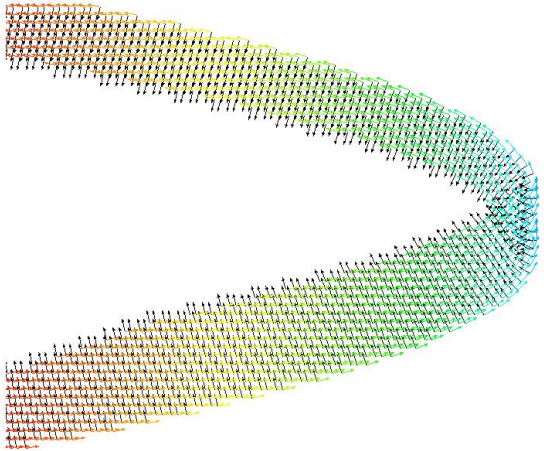

Beams interacting in a medim with
$\mathrm{Im}(K) = 0$ and $\mathrm{Re}(K) \neq 0$

THE POLARIZATION CONFIGURATION ON OMEGA IS NON-SYMMETRIC

Why would the polarization effect matter ... ?

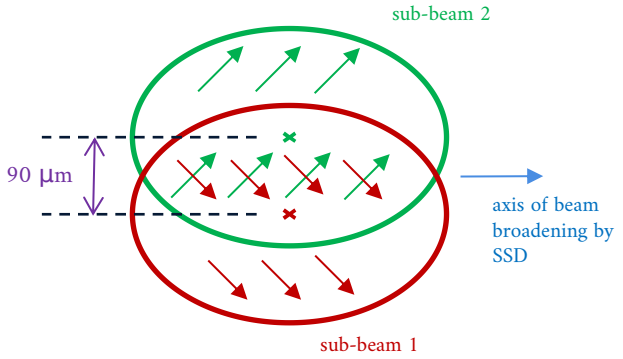

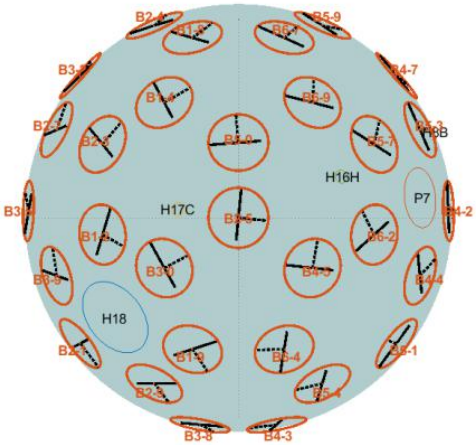

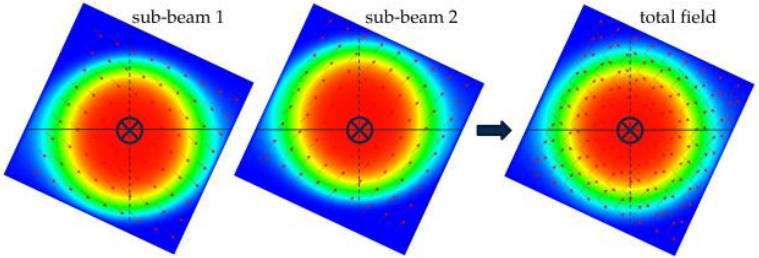

Distributed Polarization Rotators introduce a preferential axis that breaks the spherical symmetry

INLINE MODELING OF POLARIZED CBET RELIES ON DECOMPOSITION OF THE FIELD ON THE FRENET FRAME OF RAYS

Frenet reference frame

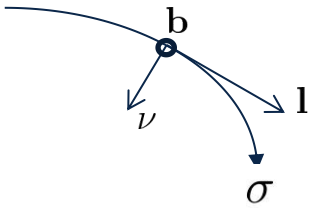

$$\boldsymbol{\nu} = \frac{1}{2\mathcal{K}\epsilon'}\nabla_\perp \epsilon'$$

$$\mathcal{K} = \frac{1}{2}\left|\frac{\nabla\epsilon'}{\epsilon'} \times \mathbf{l}\right|$$

$$\frac{\mathrm{d}\boldsymbol{\nu}}{\mathrm{d}\sigma} = -\mathcal{K}\mathbf{l} + \kappa\mathbf{b}$$

$$\kappa = \mathbf{b}.\frac{\mathrm{d}\boldsymbol{\nu}}{\mathrm{d}\sigma}$$

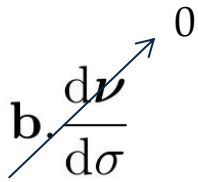

INLINE MODELING OF POLARIZED CBET RELIES ON DECOMPOSITION OF THE FIELD ON THE FRENET FRAME OF RAYS

Frenet reference frame

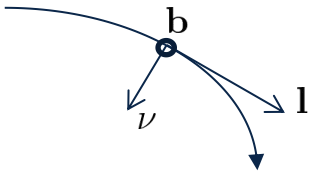

$$\boldsymbol{\nu} = \frac{1}{2\mathcal{K}\epsilon'}\nabla_\perp \epsilon'$$

$$\mathcal{K} = \frac{1}{2}\left|\frac{\nabla\epsilon'}{\epsilon'} \times \mathbf{l}\right|$$

$$\frac{\mathrm{d}\boldsymbol{\nu}}{\mathrm{d}\sigma} = -\mathcal{K}\mathbf{l} + \kappa\mathbf{b}$$

$$\kappa = \mathbf{b}.\frac{\mathrm{d}\boldsymbol{\nu}}{\mathrm{d}\sigma}$$

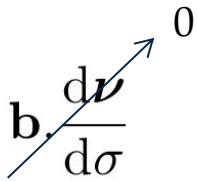

$$\frac{\partial \mathbf{a}_1}{\partial \mathbf{l}_1} = \frac{\imath}{8k_1} K_{10} k_{b,10}^2 (\mathbf{a}_0^\star.\mathbf{a}_1)\mathbf{a}_0$$

$$\frac{\partial \mathbf{a}_0}{\partial \mathbf{l}_0} = \frac{\imath}{8k_0} K_{01} k_{b,01}^2 (\mathbf{a}_0.\mathbf{a}_1^\star)\mathbf{a}_1$$

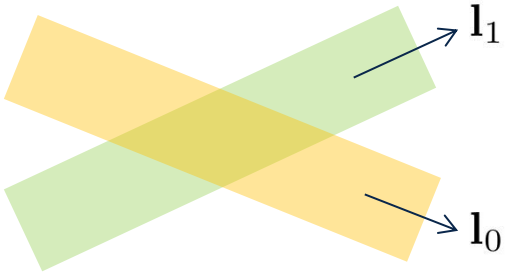

Coupling eqs. between 3D complex fields

INLINE MODELING OF POLARIZED CBET RELIES ON DECOMPOSITION OF THE FIELD ON THE FRENET FRAME OF RAYS

Frenet reference frame

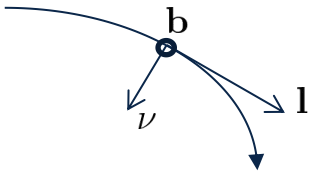

$$\boldsymbol{\nu} = \frac{1}{2\mathcal{K}\epsilon'}\nabla_\perp \epsilon' \qquad \mathcal{K} = \frac{1}{2}\left|\frac{\nabla\epsilon'}{\epsilon'} \times \mathbf{l}\right|$$

$$\frac{\mathrm{d}\boldsymbol{\nu}}{\mathrm{d}\sigma} = -\mathcal{K}\mathbf{l} + \kappa\mathbf{b} \qquad \kappa = \mathbf{b}.\frac{\mathrm{d}\boldsymbol{\nu}}{\mathrm{d}\sigma}$$

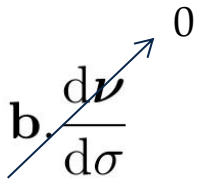

Complex s/p components in the Frenet frame

$$\frac{\partial}{\partial \mathbf{l}_n}\begin{pmatrix} a_{n,\nu_n} \\ a_{n,b_n} \end{pmatrix} = \underline{\underline{\mathcal{D}_n}}.\begin{pmatrix} a_{n,\nu_n} \\ a_{n,b_n} \end{pmatrix}$$

$$\frac{\partial \mathbf{a}_1}{\partial \mathbf{l}_1} = \frac{\imath}{8k_1}K_{10}k_{b,10}^2(\mathbf{a}_0^\star.\mathbf{a}_1)\mathbf{a}_0$$

$$\frac{\partial \mathbf{a}_0}{\partial \mathbf{l}_0} = \frac{\imath}{8k_0}K_{01}k_{b,01}^2(\mathbf{a}_0.\mathbf{a}_1^\star)\mathbf{a}_1$$

$$\longrightarrow \quad \underline{\underline{\mathcal{D}_n}} = \frac{\imath}{8k_n}\sum_{\substack{m\in\text{beams,sheets} \\ m\neq n}} K_{nm}^\star k_{b,nm}^2 \underline{\underline{\mathbf{M_{nm}}}}$$

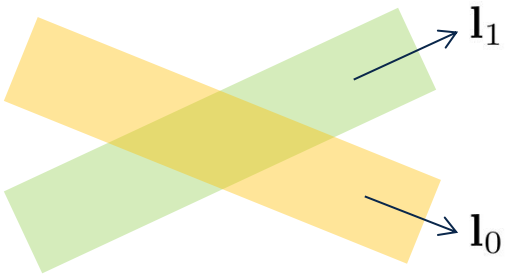

Complex kinetic plasma response
Langdon and Dewandre effect
Real part: induces ellipticity
Imaginary part: depletion or gain

INLINE MODELING OF POLARIZED CBET RELIES ON DECOMPOSITION OF THE FIELD ON THE FRENET FRAME OF RAYS

Frenet reference frame

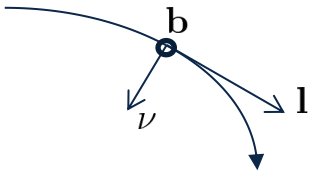

$$\boldsymbol{\nu} = \frac{1}{2\mathcal{K}\epsilon'}\nabla_\perp \epsilon' \qquad \mathcal{K} = \frac{1}{2}\left|\frac{\nabla\epsilon'}{\epsilon'} \times \mathbf{l}\right|$$

$$\frac{\mathrm{d}\boldsymbol{\nu}}{\mathrm{d}\sigma} = -\mathcal{K}\mathbf{l} + \kappa\mathbf{b} \qquad \kappa = \mathbf{b}.\frac{\mathrm{d}\boldsymbol{\nu}}{\mathrm{d}\sigma}$$

0

Complex s/p components in the Frenet frame

$$\frac{\partial}{\partial \mathbf{l}_n}\begin{pmatrix} a_{n,\nu_n} \\ a_{n,b_n} \end{pmatrix} = \underline{\underline{\mathcal{D}_n}}.\begin{pmatrix} a_{n,\nu_n} \\ a_{n,b_n} \end{pmatrix}$$

$$\frac{\partial \mathbf{a}_1}{\partial \mathbf{l}_1} = \frac{\imath}{8k_1}K_{10}k_{b,10}^2(\mathbf{a}_0^\star.\mathbf{a}_1)\mathbf{a}_0$$
$$\frac{\partial \mathbf{a}_0}{\partial \mathbf{l}_0} = \frac{\imath}{8k_0}K_{01}k_{b,01}^2(\mathbf{a}_0.\mathbf{a}_1^\star)\mathbf{a}_1$$

$$\longrightarrow \quad \underline{\underline{\mathcal{D}_n}} = \frac{\imath}{8k_n}\sum_{\substack{m\in\text{beams,sheets}\\ m\neq n}}^{N} K_{nm}^\star k_{b,nm}^2 \underline{\underline{\mathbf{M_{nm}}}}$$

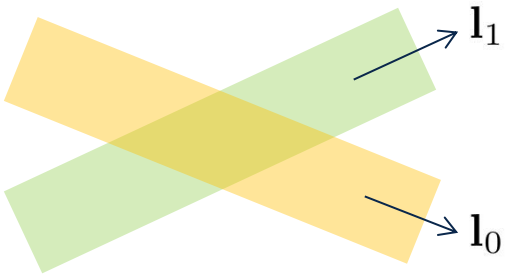

$$\underline{\underline{\mathbf{M_{nm}}}} = \begin{pmatrix} a_{m,\nu_n}^2 & a_{m,b_n}^\star a_{m,\nu_n} \\ a_{m,b_n} a_{m,\nu_n}^\star & a_{m,b_n}^2 \end{pmatrix}$$

Matrix responsible for polarization rotation and ellipticity

"Usual" coupling

$$\begin{pmatrix} \epsilon_{i,j,\nu_n} \\ \epsilon_{i,j,b_n} \end{pmatrix} = [\epsilon_i' + \imath(\epsilon_{0,i}'' f_\mathrm{L} + \underline{\underline{\mathcal{D}_{i,j}}})].\begin{pmatrix} 1 \\ 1 \end{pmatrix}$$

Coupling eqs. between 3D complex fields

Each polarization component sees a different permittivity

INLINE MODELING OF POLARIZED CBET RELIES ON DECOMPOSITION OF THE FIELD ON THE FRENET FRAME OF RAYS

Frenet reference frame

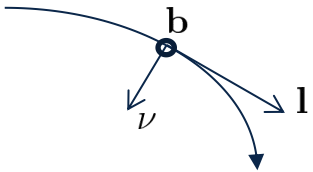

$$\boldsymbol{\nu} = \frac{1}{2\mathcal{K}\epsilon'}\nabla_\perp \epsilon' \qquad \mathcal{K} = \frac{1}{2}\left|\frac{\nabla\epsilon'}{\epsilon'} \times \mathbf{l}\right|$$

$$\frac{\mathrm{d}\boldsymbol{\nu}}{\mathrm{d}\sigma} = -\mathcal{K}\mathbf{l} + \kappa\mathbf{b} \qquad \kappa = \mathbf{b}.\frac{\mathrm{d}\boldsymbol{\nu}}{\mathrm{d}\sigma}$$

0

Complex s/p components in the Frenet frame

$$\frac{\partial}{\partial \mathbf{l}_n}\begin{pmatrix} a_{n,\nu_n} \\ a_{n,b_n} \end{pmatrix} = \underline{\underline{\mathcal{D}_n}}.\begin{pmatrix} a_{n,\nu_n} \\ a_{n,b_n} \end{pmatrix}$$

$$\frac{\partial \mathbf{a}_1}{\partial \mathbf{l}_1} = \frac{\imath}{8k_1}K_{10}k_{b,10}^2(\mathbf{a}_0^\star.\mathbf{a}_1)\mathbf{a}_0$$

$$\frac{\partial \mathbf{a}_0}{\partial \mathbf{l}_0} = \frac{\imath}{8k_0}K_{01}k_{b,01}^2(\mathbf{a}_0.\mathbf{a}_1^\star)\mathbf{a}_1$$

$$\longrightarrow \quad \underline{\underline{\mathcal{D}_n}} = \frac{\imath}{8k_n}\sum_{\substack{m\in\text{beams,sheets} \\ m\neq n}}^{N} K_{nm}^\star k_{b,nm}^2 \underline{\underline{\mathbf{M_{nm}}}}$$

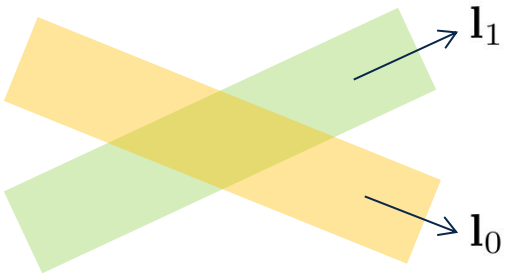

$$\underline{\underline{\mathbf{M_{nm}}}} = \begin{pmatrix} a_{m,\nu_n}^2 & a_{m,b_n}^\star a_{m,\nu_n} \\ a_{m,b_n} a_{m,\nu_n}^\star & a_{m,b_n}^2 \end{pmatrix}$$

"Usual" coupling

Matrix responsible for polarization rotation and ellipticity

Coupling eqs. between 3D complex fields

The Polarized model requires 8x more computations than the standard "unpolarized" model (2 DPR components x 2 polarization components x 2 {real + imaginary})

THE UNPOLARIZED CBET ON OMEGA INDUCES NO SIGNIFICANT ASSYMETRY ON THE ENERGY DEPOSITION

Heat source calculated in a 1D hydro profile - no CBET

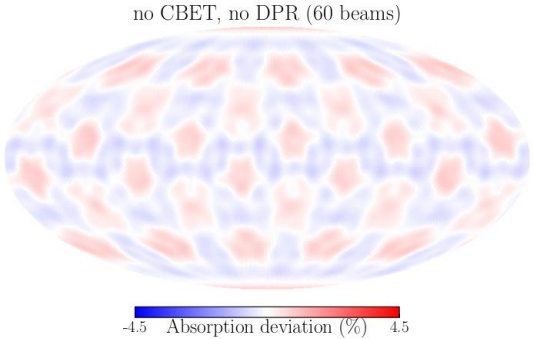

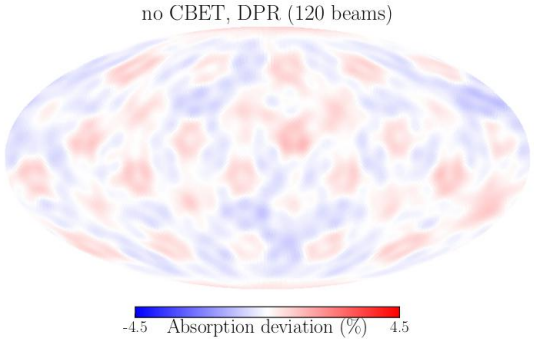

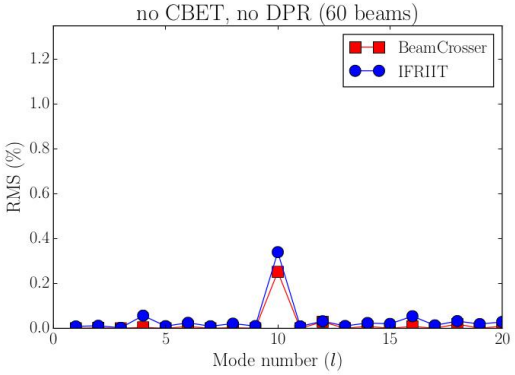

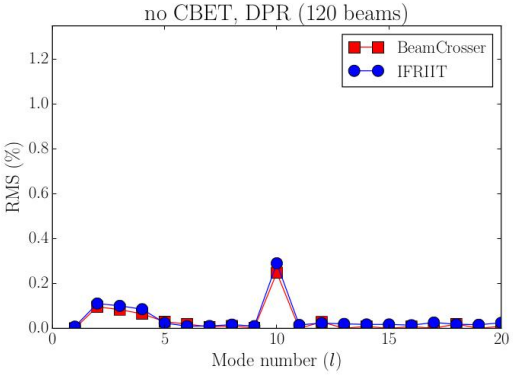

The DPR system itself induces slight low modes, small effect

THE POLARIZED CBET INDUCES A NON-NEGLIGIBLE LOW MODE ANOMALY ON THE ENERGY DEPOSITION PATTERN

Heat source calculated in a 1D hydro profile - CBET

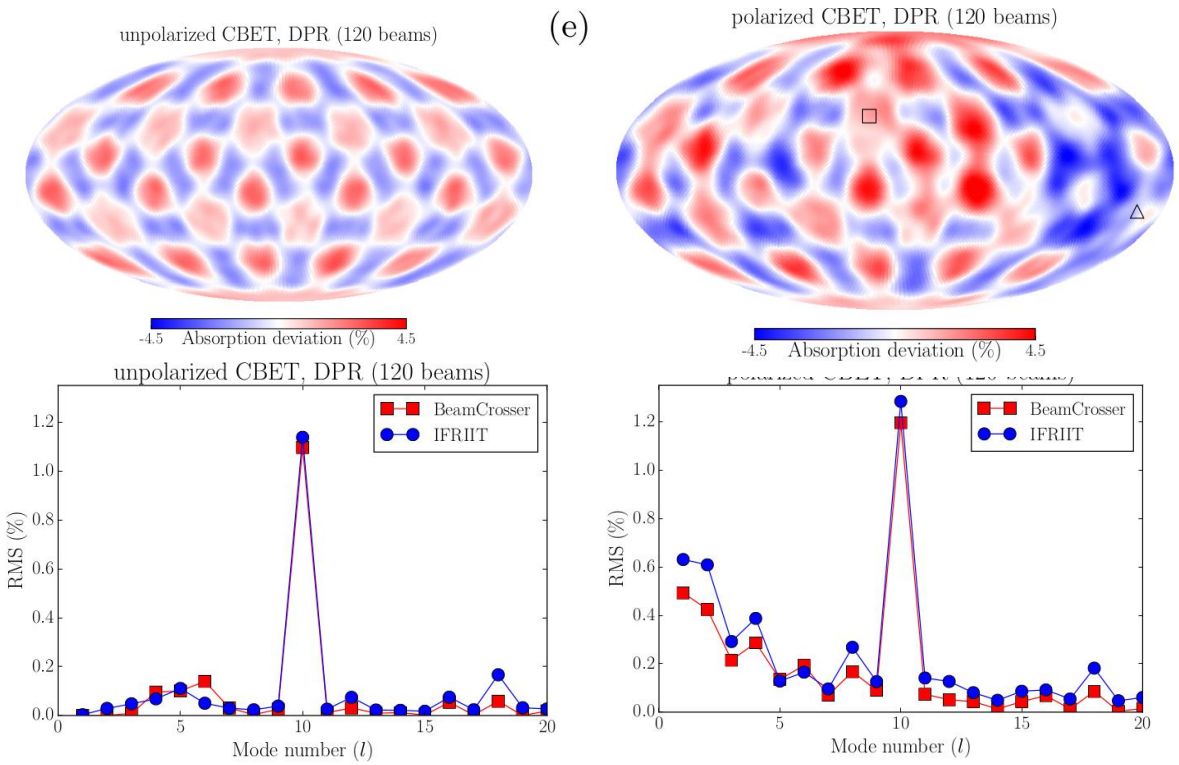

The polarization effect induces significant low modes

Consistent with results from D. Edgell obtained using BeamletCrosser postprocessor

What is the compound effect accounting for hydrodynamics feedback and other low mode sources ?

THE ASTER+IFRIIT COUPLED CODE WAS DEVELOPPED TO STUDY ICF IMPLOSIONS CONSIDERING MOST LOW MODE SOURCES

ASTER 3-D radiative hydrodynamics code
- Eulerian spherical moving grid
- EOS, heat transport, radiation, hydro...
- High resolution, block-decomposed MPI

[I. V. Igumenshchev et al. PoP (2016), I. V. Igumenshchev et al. PoP (2017)]

ASTER+IFRIIT code coupling
[A. Colaïtis, I. V. Igumenshchev et al. JCP (2021)]

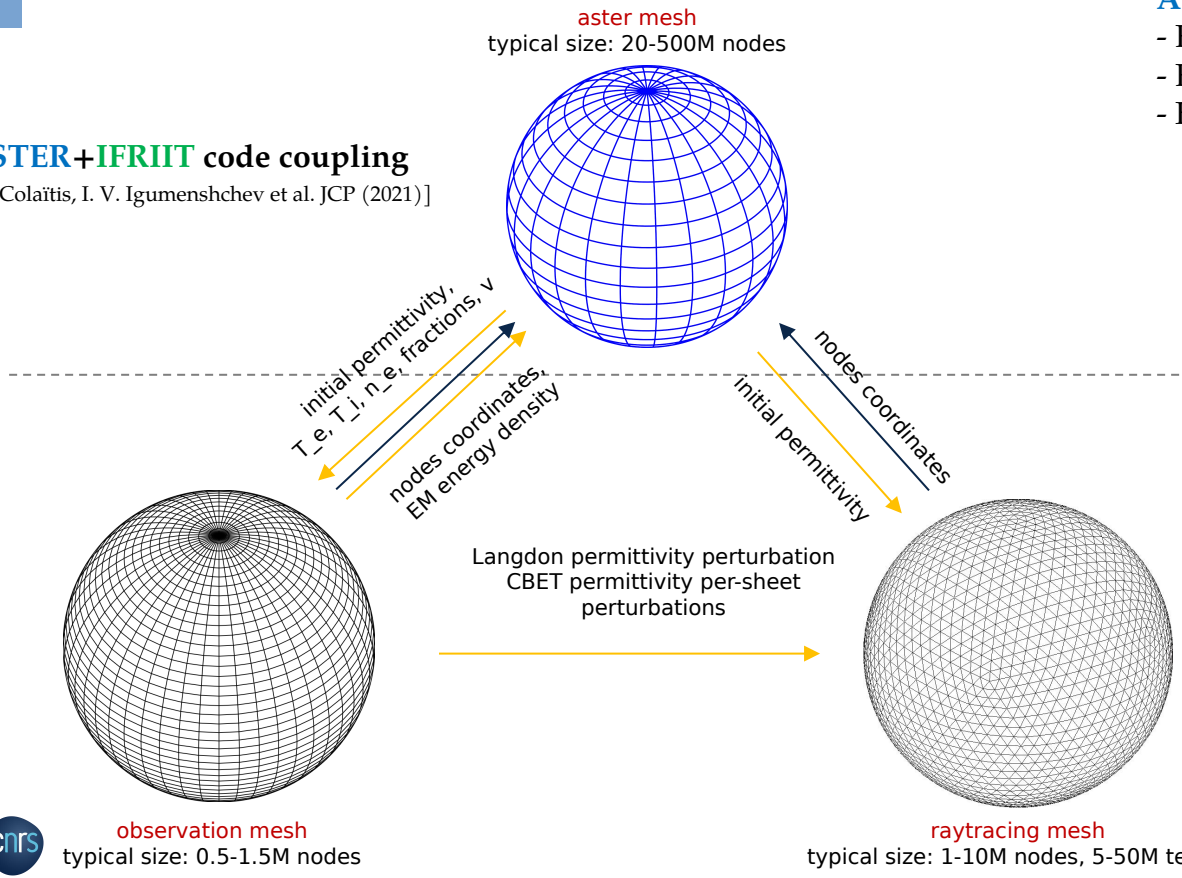

IFRIIT 3-D laser propagation code
- Inverse Ray Tracing for fast and low noise field computations
- Caustic modeling with Etalon Integrals
- CBET with many physics models, including polarization
- Adaptive resolution, domain-duplicated MPI/OpenMP

[A. Colaïtis et al., PoP 26(3) (2019), A. Colaïtis et al., PoP 26(7) (2019)]

WE STUDY 4 SHOTS CONSIDERING MOST LOW MODE SOURCES

Shot number	Date	Type	E_{las} (kJ)	D_t (μm)	Offset magnitude (μm)	Pointing shot	Pointing $l=1$ (% RMS)	Balance $l=1$ (% RMS) picket	early drive	late drive
94343	09/07/2019	cryo	27.7	982	3.5	94336	1.26	2.58	0.48	1.45
94712	09/08/2019	cryo	28.4	961.4	7.0*	94708	5.94	4.52	0.35	1.34
98768	27/10/2020	cryo	28.4	1012	3.2	98762	1.08	1.72	0.43	1.7
98755	26/10/2020	warm	27.9	978.2	1.3	98754/98757	0.64/1.0	0.71	0.79	0.92

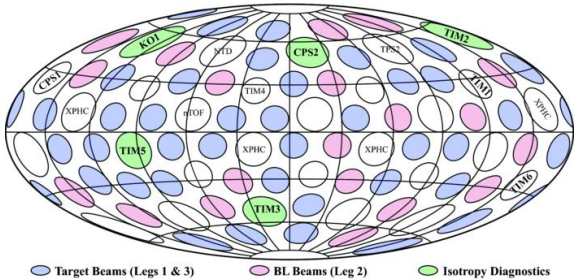

OMEGA detailed beam geometry
120 DPR-split beams

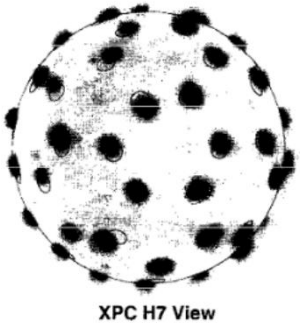

Measured beam pointing (from begining and/or end of shot day)

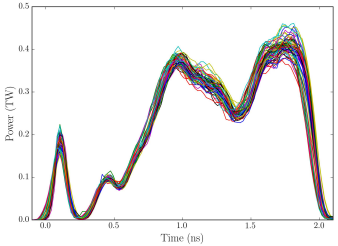

Measured pulse shapes

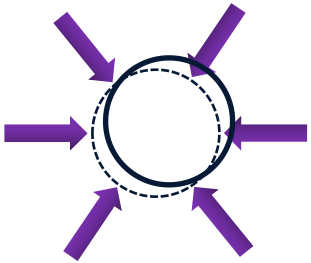

Measured offset (if available)

Important note: contrary to most inline approaches, the CBET model here has no “ad-hoc” parameter => thanks to the caustic modeling. No IAW saturation is assumed.

THE 3D MODELING REPRODUCES THE EXPERIMENTALLY MEASURED BANG TIME AND NEUTRON YIELD

Simulation results presented for 4 shots are studied ; 3 cryogenic and one « warm » shot
Total ~ 60M CPU hours of computation

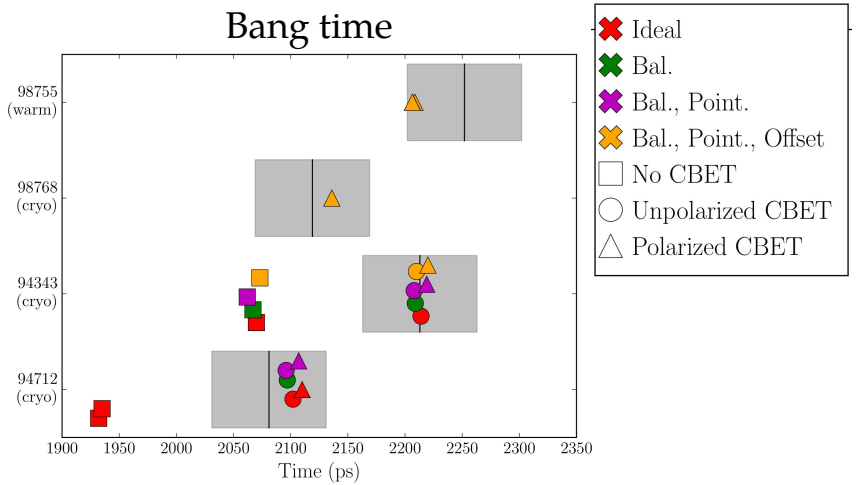

THE 3D MODELING REPRODUCES THE EXPERIMENTALLY MEASURED BANG TIME AND NEUTRON YIELD

Simulation results presented for 4 shots are studied ; 3 cryogenic and one « warm » shot
Total ~ 60M CPU hours of computation

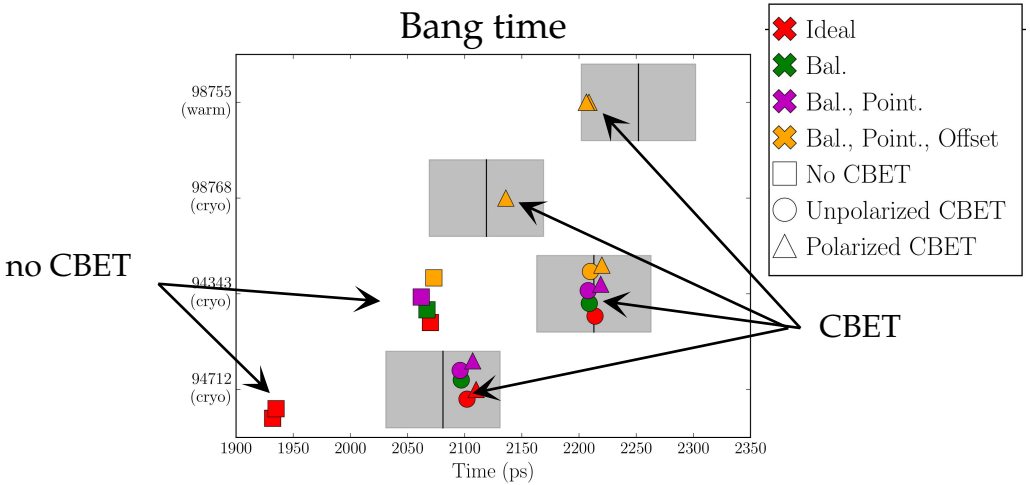

(i) The CBET model alone gets the nuclear bang time correct (drive energetics is well modeled)

THE 3D MODELING REPRODUCES THE EXPERIMENTALLY MEASURED BANG TIME AND NEUTRON YIELD

Simulation results presented for 4 shots are studied ; 3 cryogenic and one « warm » shot
Total ~ 60M CPU hours of computation

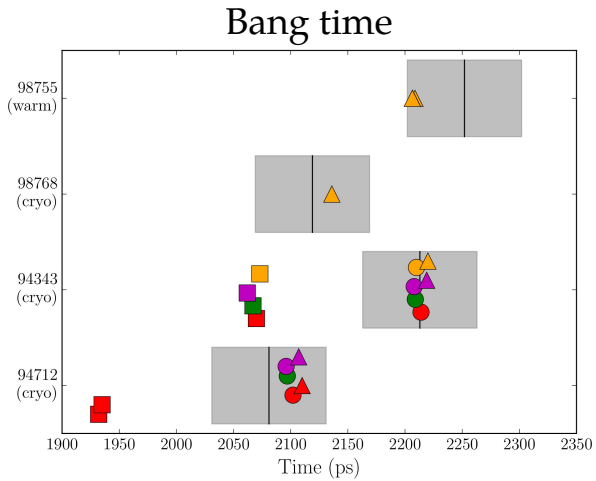

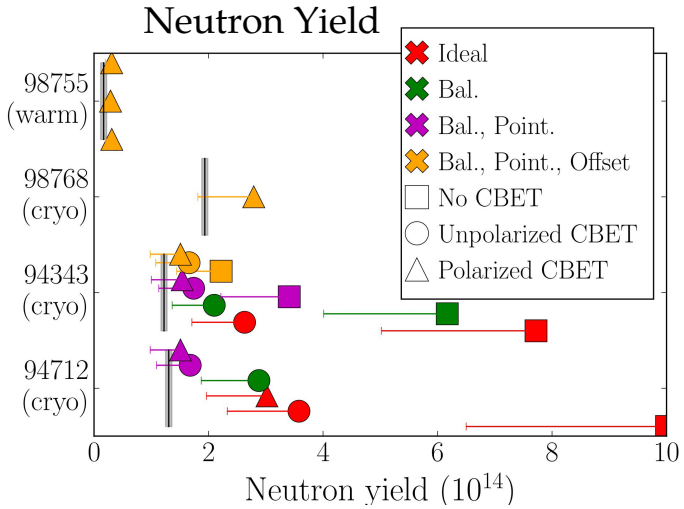

(i) The CBET model alone gets the nuclear bang time correct (drive energetics is well modeled)

Note:
- experimental yields are corrected for fuel aging (tritium decay, 3He contamination and radiological capsule damage)
- simulated yield include a “range” accounting for some of the high modes contributions

THE 3D MODELING REPRODUCES THE EXPERIMENTALLY MEASURED BANG TIME AND NEUTRON YIELD

Simulation results presented for 4 shots are studied ; 3 cryogenic and one « warm » shot
Total ~ 60M CPU hours of computation

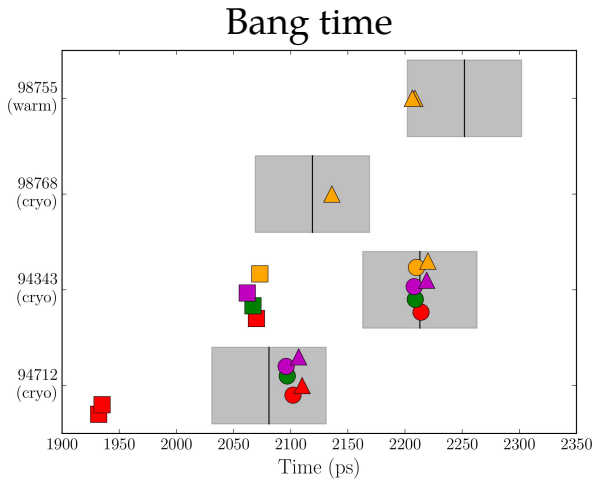

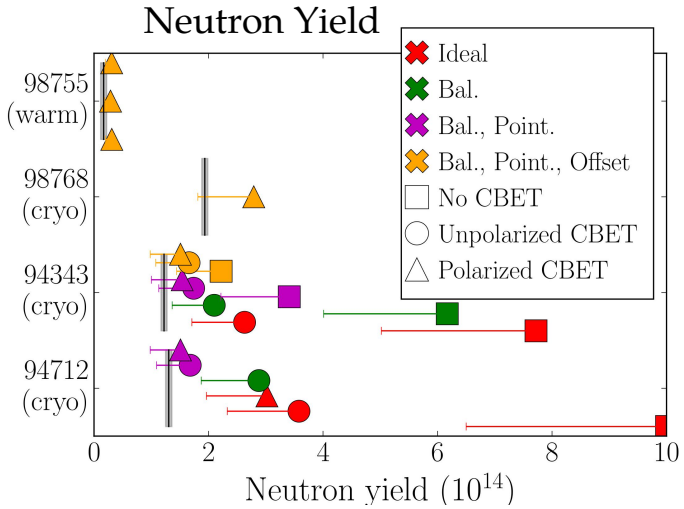

(i) The CBET model alone gets the nuclear bang time correct (drive energetics is well modeled)
(ii) CBET simulations with power balance and pointing variation get the neutron yield correctly because both drive energetics and symmetry are important to the yield

Note:
- experimental yields are corrected for fuel aging (tritium decay, 3He contamination and radiological capsule damage)
- simulated yield include a “range” accounting for some of the high modes contributions

THE 3D MODELING REPRODUCES THE EXPERIMENTALLY MEASURED BANG TIME AND NEUTRON YIELD

Simulation results presented for 4 shots are studied ; 3 cryogenic and one « warm » shot
Total ~ 60M CPU hours of computation

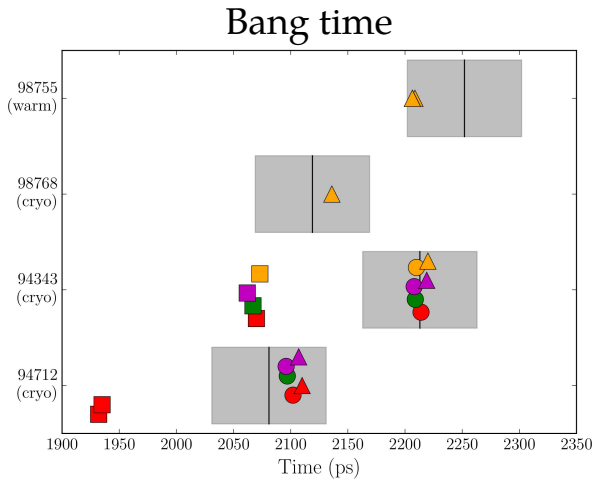

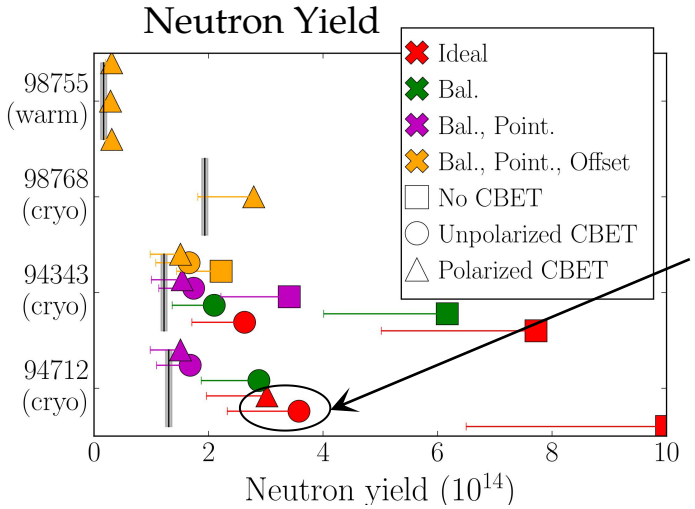

Polarization alone causes a 15% yield drop

(i) The CBET model alone gets the nuclear bang time correct (drive energetics is well modeled)
(ii) CBET simulations with power balance and pointing variation get the neutron yield correctly because both drive energetics and symmetry are important to the yield

Note:
- experimental yields are corrected for fuel aging (tritium decay, 3He contamination and radiological capsule damage)
- simulated yield include a “range” accounting for some of the high modes contributions

THE 3D MODELING ALSO APPROACHES WELL THE FLOW VELOCITY MAGNITUDE AND DIRECTION

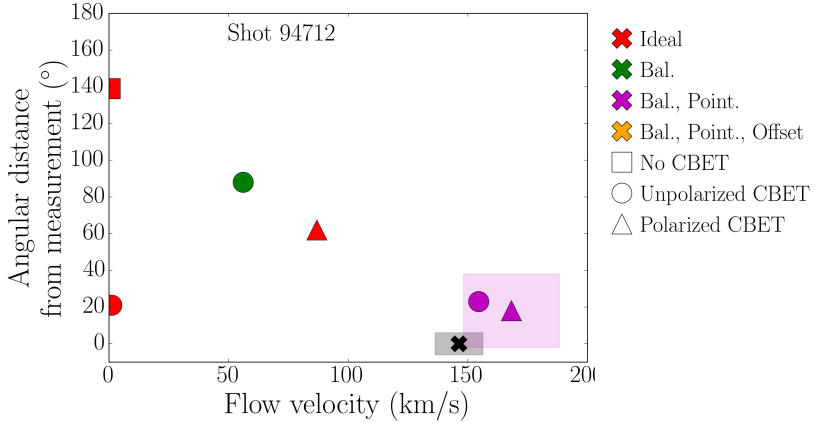

(iii) CBET with power balance and pointing variations match the flow velocity vector for 94712 because the large pointing error dominates the low mode sources

THE 3D MODELING ALSO APPROACHES WELL THE FLOW VELOCITY MAGNITUDE AND DIRECTION

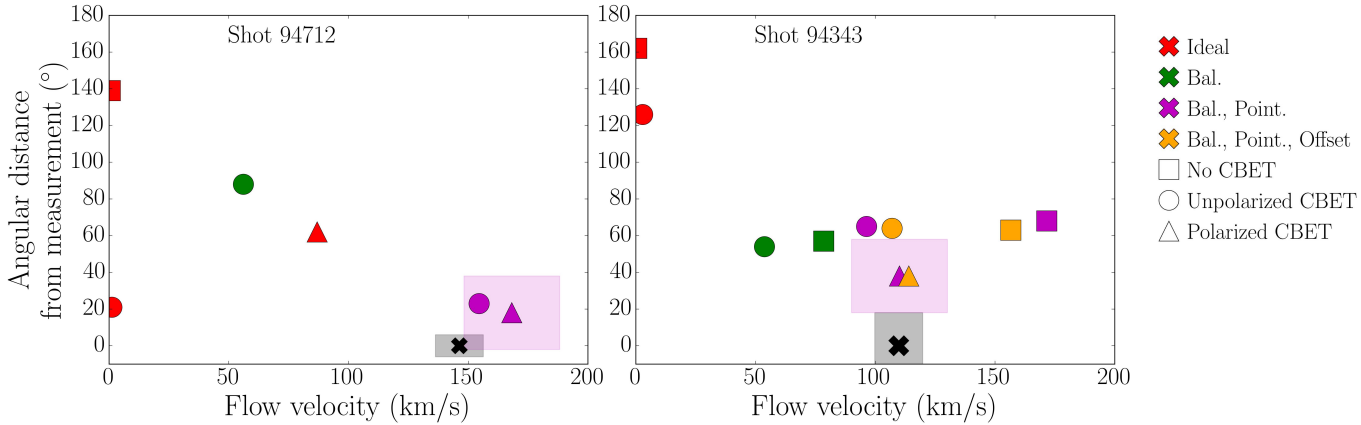

(iii) CBET with power balance and pointing variations match the flow velocity vector for 94712 because the large pointing error dominates the low mode sources

(iv) Polarized CBET with power balance and pointing is needed to get the flow velocity correctly for the more accurately pointed shot 94343 => the polarization effect begins to be more important as other low mode sources become smaller

THE 3D MODELING ALSO APPROACHES WELL THE FLOW VELOCITY MAGNITUDE AND DIRECTION

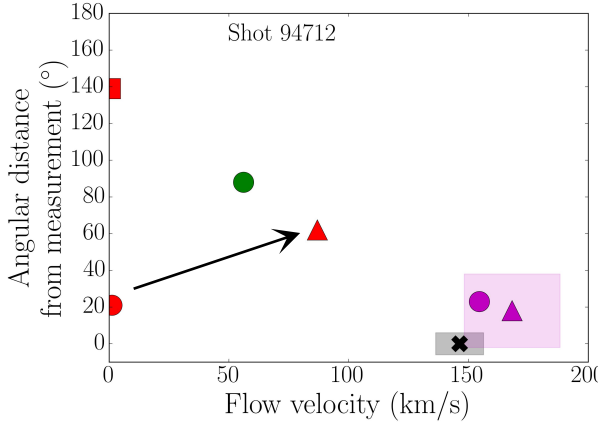

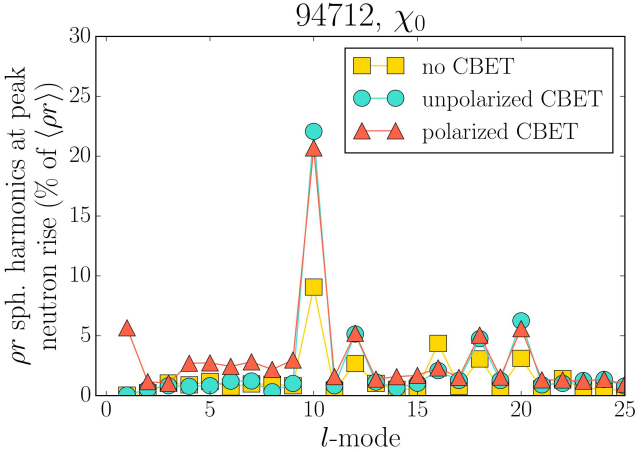

(iii) CBET with power balance and pointing variations match the flow velocity vector for 94712 because the large pointing error dominates the low mode sources
(iv) Polarized CBET with power balance and pointing is needed to get the flow velocity correctly for the more accurately pointed shot 94343 => the polarization effect begins to be more important as other low mode sources become smaller

Note the single effect of polarized CBET, that induces a ~80 km/s flow in the ideal case

SIMULATION OF LASER-TARGET COUPLING EXPERIMENTS ON THE NIF SHOWS THAT THE MODELING ALSO CAPTURES DRIVE AT NIF SCALE

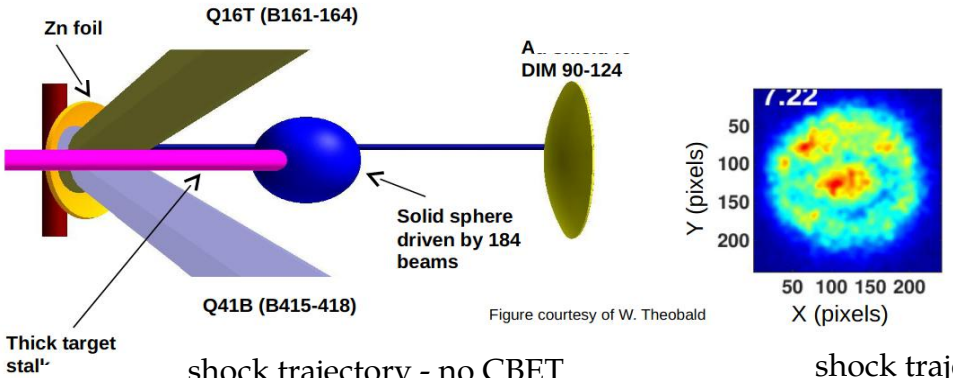

Figure courtesy of W. Theobald

shock trajectory - no CBET

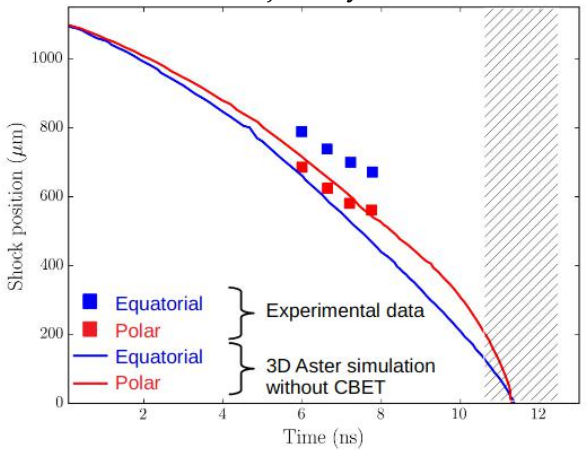

shock trajectory - CBET

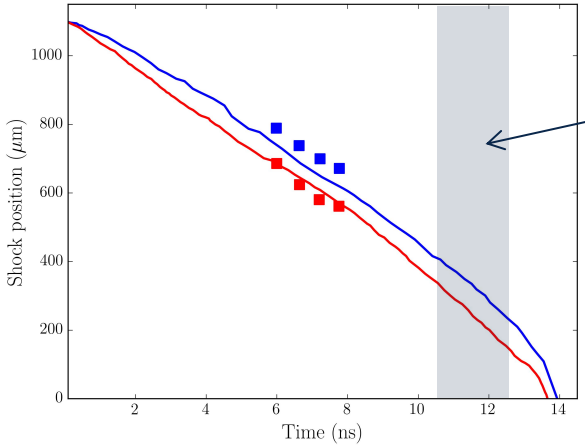

region where no shock flash was observed in the data

[D. Viala, manuscript in prep.]

The modeling also captures drive energetics correctly for NIF scale shock coupling experiments

THE CURRENT BEST PERFORMANCES OF THE LASER SYSTEM CAN STILL CAUSE HIGHLY SIGNIFICANT FLOW ANOMALIES

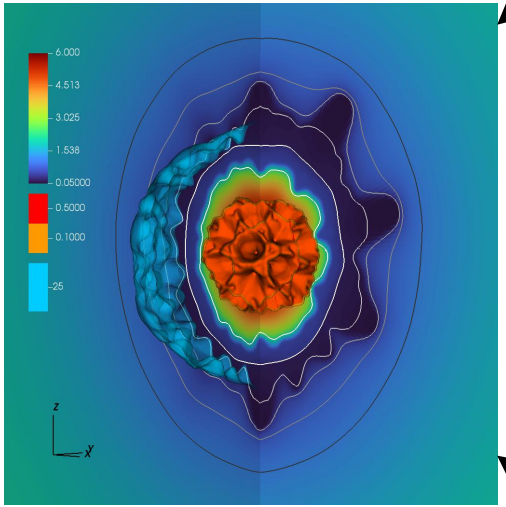

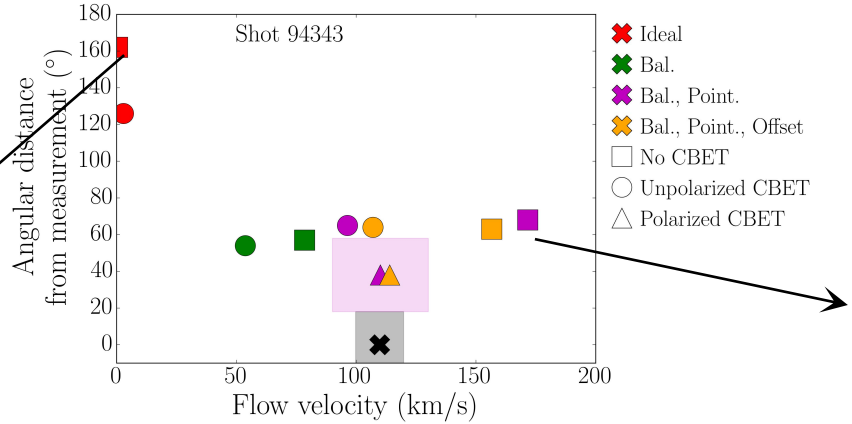

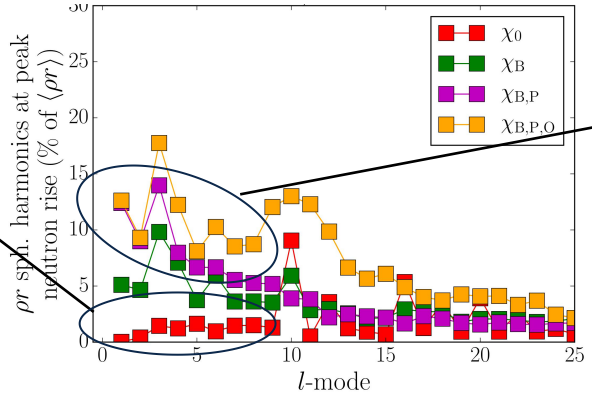

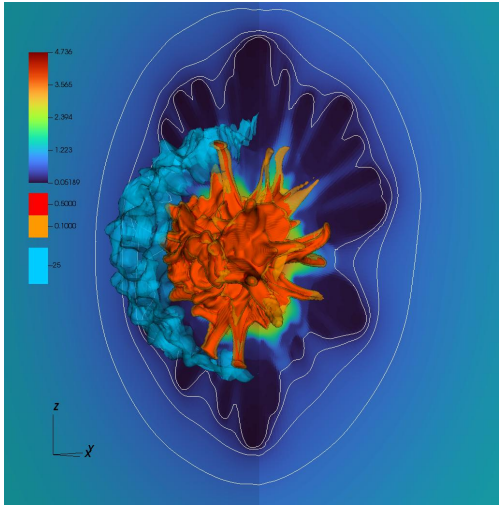

Without CBET, best levels of pointings, balance and offset introduce significant low modes at stagnation, with **DT flows that can reach up to 170 km/s**

THE CURRENT BEST PERFORMANCES OF THE LASER SYSTEM CAN STILL CAUSE HIGHLY SIGNIFICANT FLOW ANOMALIES

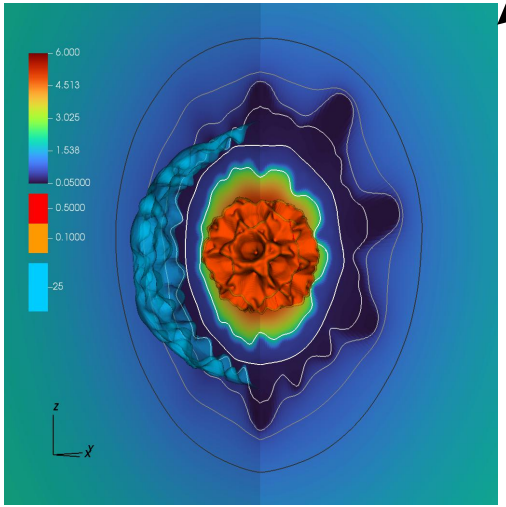

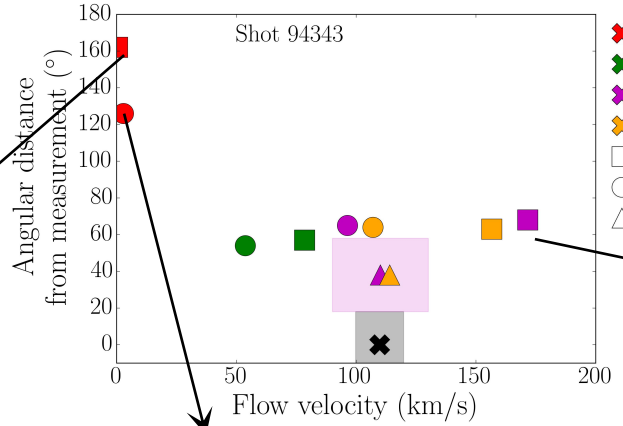

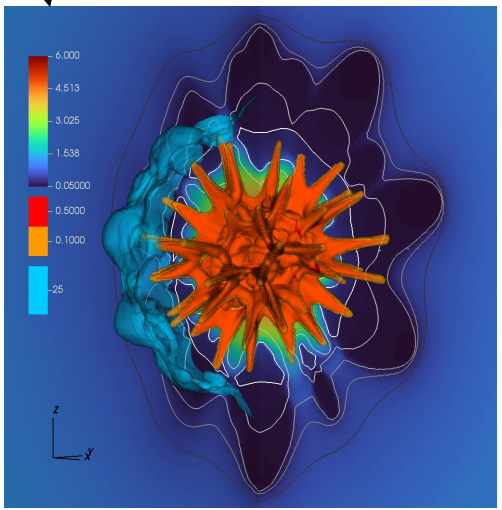

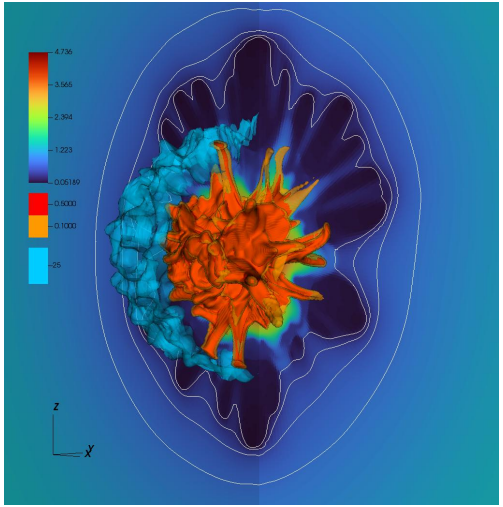

In ideal conditions, CBET amplifies mode 10 sufficiently to lead to target perforation

YIELD IS STRONGLY DRIVEN BY CBET AND SYSTEM LOW MODES

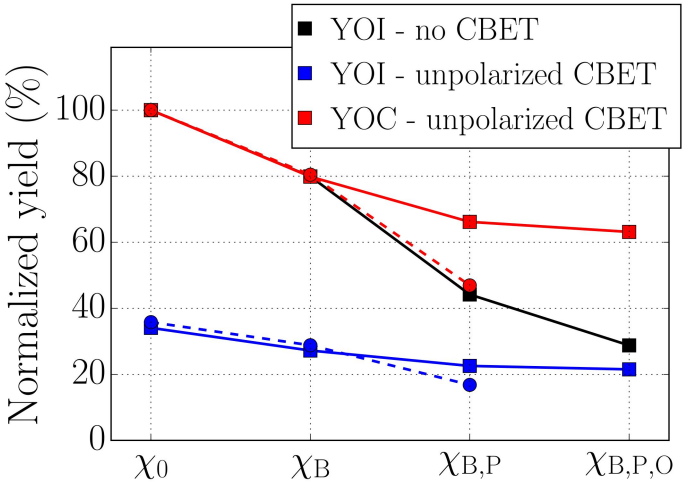

solid: 94343
dashed: 94712

- **CBET** alone **reduces neutron yields by ~60 %** in the ideal case → a realistic fusion driver must remove CBET
- **System-induced low modes are mitigated by CBET** → designs without CBET must be made more robust to low modes

=> How to mitigate low modes ? We can explore two mitigation strategies (current and envisonned)

MITIGATION OF LOW MODES BY TARGET OFFSET CAN ONLY RECOVER A FINITE AMOUNT OF YIELD

Strategy 1 : offset mitigation
- In experiments, the target can be offset opposite to the direction of the measured flow anomaly (this is used routinely to improve yields)
Pros : Simple to implement, allows to recover ~15 % in yield at maximum here
Cons : The method rapidly reachs a maximum efficacy due to it mitigating only l=1. In particular, even in the ideal case, polarized CBET introduces other modes than l=1. It is also a post-hoc method.

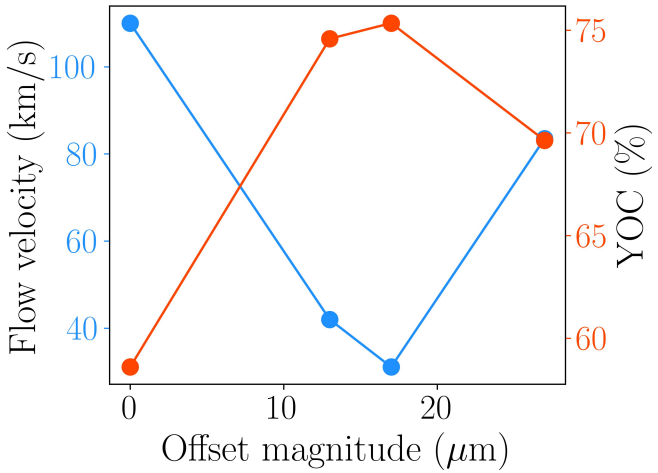

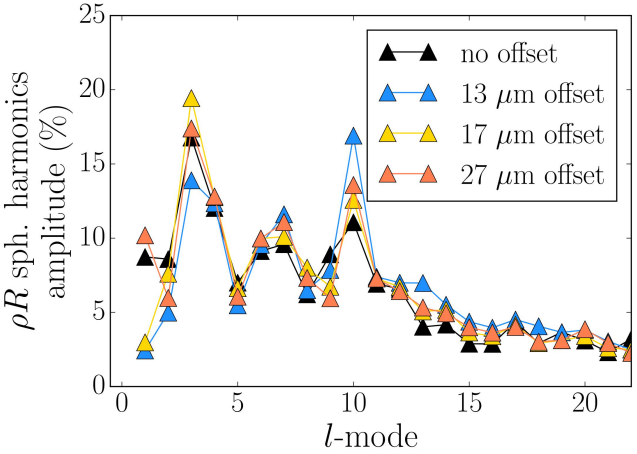

A RE-DESIGN OF THE OMEGA DPR SYSTEM IS A MORE VIABLE LONG TERM STRATEGY TO IMPROVE IMPLOSION PERFORMANCE

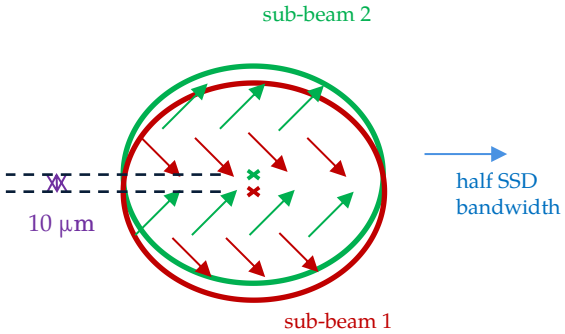

Strategy 2 :
- Re-design the DPR system on OMEGA to reduce the offset between polarizations
Pros : Allows to recover the unpolarized CBET result, effectively mitigating this source of low modes
Cons : difficult to implement, also requires to half the SSD bandwidth...

However, this anomaly does need to be corrected in the long run ...

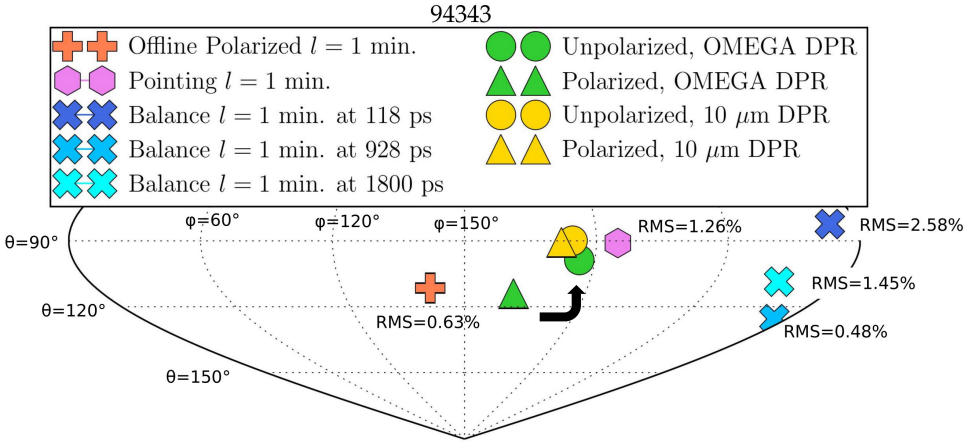

A LINE-BASED INLINE CBET MODEL HAS BEEN IMPLEMENTED IN ASTER/IFRIIT

Recall: **CBET** alone **reduces neutron yields by ~60 %** in the ideal case

Bandwidth has been proposed as a way to mitigate CBET.

A ray-based bandwidth CBET model was implemented in IFRIIT*: the spectrum is discretized in lines for which power is tracked along the rays. The modeling was validated against LPSE.

$$\delta\epsilon_{ij} = \frac{\chi_{i,j}c^2}{4\omega_{\mathrm{pe}}^2}\left[\sum_{\substack{l\in\mathrm{beams}\\ m\in\mathrm{sheets}}} |\mathbf{k}_{ij}-\mathbf{k}_{lm}|^2|u_{lm}|^2K_{lm} + \sum_{\substack{m\in\mathrm{sheets}\\ m\neq j}} |\mathbf{k}_{ij}-\mathbf{k}_{im}|^2|u_{im}|^2K_{im}\right]$$

$$\delta\epsilon_{ij} = \frac{\chi_{i,j}c^2}{4\omega_{\mathrm{pe}}^2}\left[\sum_{\substack{l\in\mathrm{beams}\\ m\in\mathrm{sheets}\\ n\in\mathrm{lines}}} |\mathbf{k}_{ij}-\mathbf{k}_{lm}|^2|u_{lmn}|^2K_{lmn} + \sum_{\substack{m\in\mathrm{sheets}\\ m\neq j\\ n\in\mathrm{lines}}} |\mathbf{k}_{ij}-\mathbf{k}_{im}|^2|u_{imn}|^2K_{imn}\right]$$

Unpolarized CBET for OMEGA
(no DPR)

Track 120 wavefields
(60 beams x 2 sheets)

Track 600 wavefields

Note: a polarized calculation with bandwidth would require tracking 2400 wavefields
Note 2: recall that CBET cost scales as n_wavefields**2; bandwidth calculation with 5 lines requires 25 more CBET coefficients evaluations

*Based on the work of [R. K. Follett et al. In preparation]
** [A. G. Seaton et al. Phys. Plasma (2022)"Cross-beam energy transfer in direct-drive ICF. II. Theory and simulation of mitigation through increased laser bandwidth"]

EFFECT OF LASER BANDWIDTH ON A TYPICAL OMEGA IMPLOSION

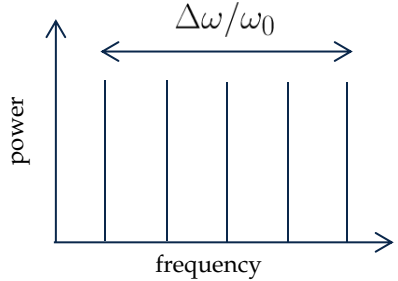

Case 94343 with 1% flat spectrum (worst-case scenario**), modeled with 5 lines:

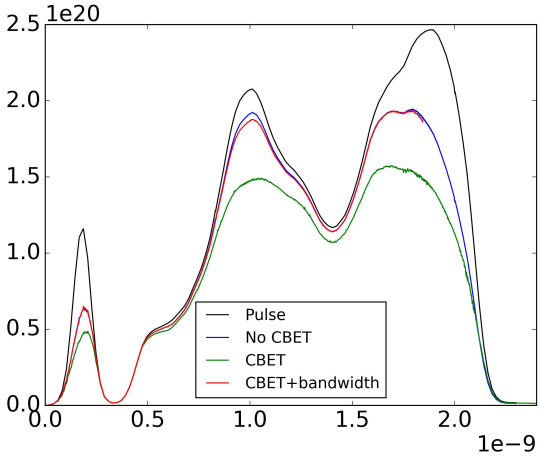

From a drive energetics point of view: efficient CBET mitigation at OMEGA scale with 1% bandwidth

EFFECT OF LASER BANDWIDTH ON A TYPICAL OMEGA IMPLOSION

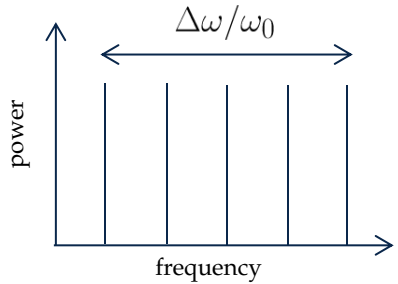

Case 94343 with 1% flat spectrum (worst-case scenario**), modeled with 5 lines:

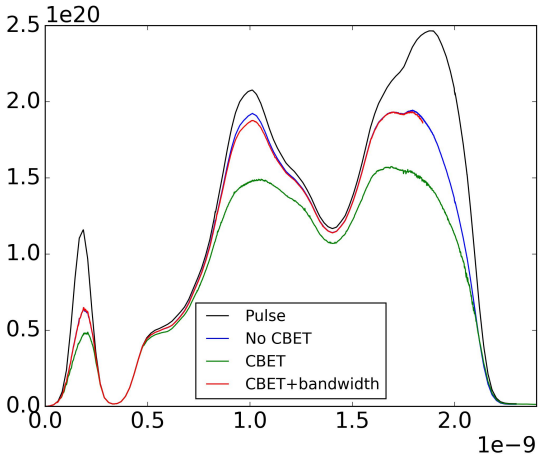

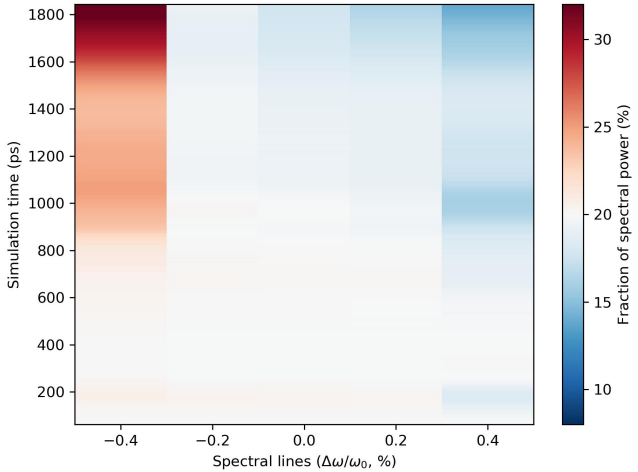

=> Scattered light spectrum skewed with red-shifted lines having up to 35% of the beam power (instead of 20%) -> reduces bandwidth efficiency but still enough

=> Same for all beams in the ideal drive case

EFFECT OF LASER BANDWIDTH ON A TYPICAL OMEGA IMPLOSION

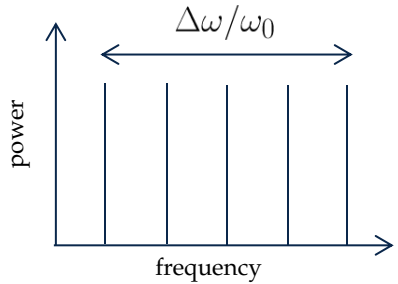

Case 94343 with 1% flat spectrum (worst-case scenario**), modeled with 5 lines:

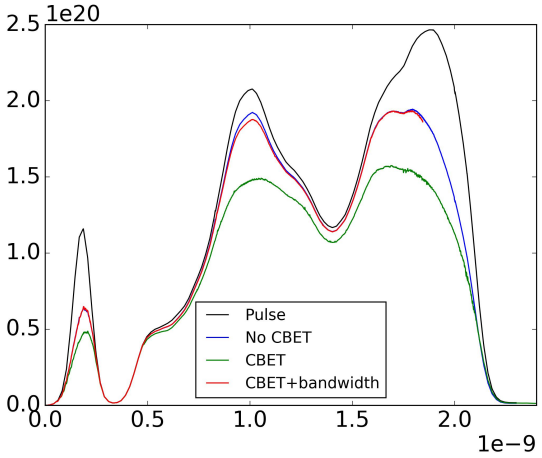

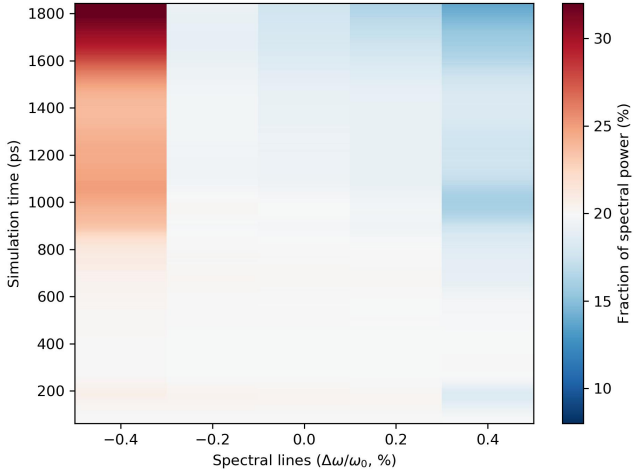

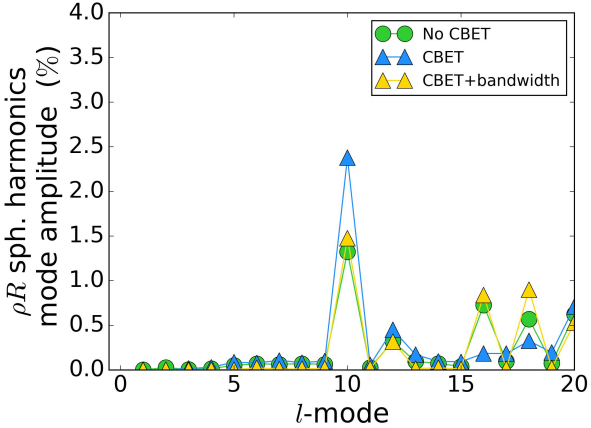

=> The CBET bandwidth cases recover the areal density modes of the no-CBET case
=> It remains to check if:
- low-modes from the drive change this picture
- this amount of bandwidth remains sufficient at ignition-scale

CONCLUSIONS AND PERSPECTIVES

Conclusions:

- The CBET models implemented in ASTER/IFRIIT reproduce the large scale dynamics of implosion experiments on OMEGA, without any tuning
- ... also holds for NIF-scale direct-drive experiments => good confidence in modeling capabilities
- Some limitations remain (stalk, high mode modeling coupled to CBET)

- Polarized CBET, in addition to current low modes, explains the observed anomaly of the last 2 years of OMEGA shots
- Polarization effect is responsible for ~15% yield drop on OMEGA and is mostly present when other low mode sources are low
- CBET reduces yields by at least 60% on OMEGA, even worse at NIF scale => must be mitigated in a fusion driver. However, this will make current designs more vulnerable to system errors -> need more robust schemes
- Preliminary 3D inline simulations confirm that 1% bandwidth fully mitigates CBET at OMEGA scale

THE MODELING SYSTEMATICALLY APPROACHES THE MEASURED FLOW DIRECTION

Good agreement in flow direction also for 98768

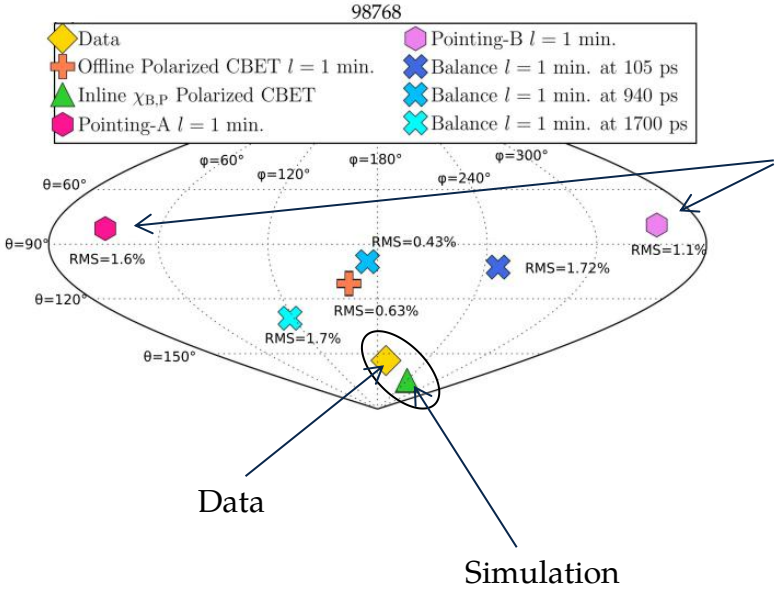

Note: 53° between two pointing analysis of the same pointing shot

For this shot, the simulation underestimates the flow velocity (72 km/s vs 133 km/s measured)

THE KNOWLEDGE OF THE ACTUAL POINTING MODES IS LIMITING OUR AGREEMENT WITH THE DATA

Note:
- 80 to 100° difference between the morning and afternoon pointing shots despite no TIM transaction

For this shot, the simulations underestimates the flow velocity (50 km/s vs 84 km/s measured)

=> Knowledge of pointing limitates our predictability of flow direction

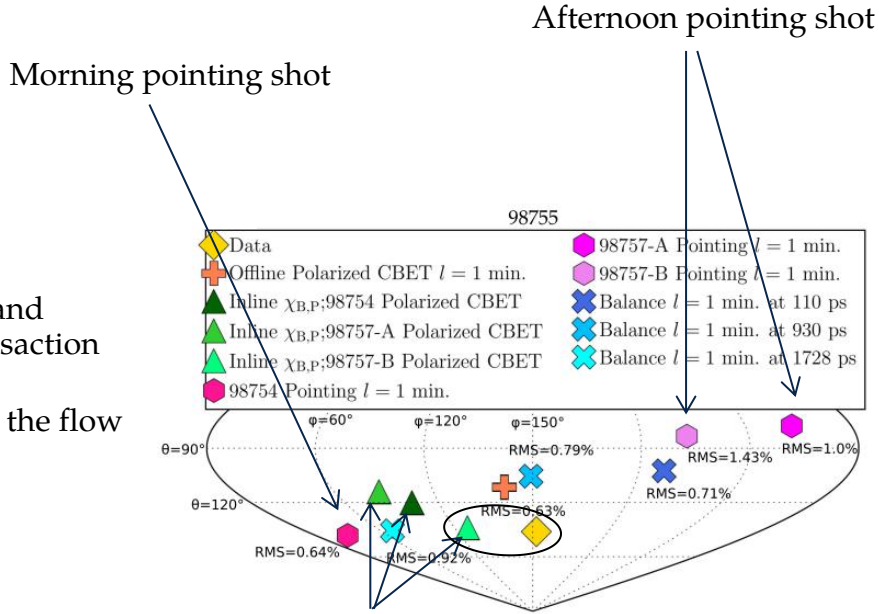

Three simulations with three pointings

REASONABLE NUMERICAL EFFICIENCY IS OBTAINED BY LEVERAGING INVERSE RAY TRACING

$$u = A\exp[ik_0\psi] \ ,$$

$$\psi''(\tau) = \int_0^\tau \epsilon''(\mathbf{r}(\hat{\tau}))\mathrm{d}\hat{\tau}/2 \ ,$$

$$A(\tau) = A(0)\left|\frac{D(0)}{D(\tau)}\right|^{1/2} \ ,$$

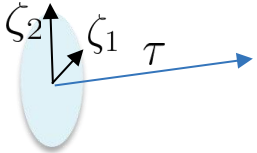

Step 1; manifold geometry
- compute the mapping from phase space (ζ_1, ζ_2) to real space (x, y)
- compute the geometric part of the laser field
- compute the Airy Integral that gives the caustic field
- compute the full Frenet frame for each sheet of each beam at each gridpoint

=> these are **geometric** factors stemming from the ray mapping fixed during one timestep

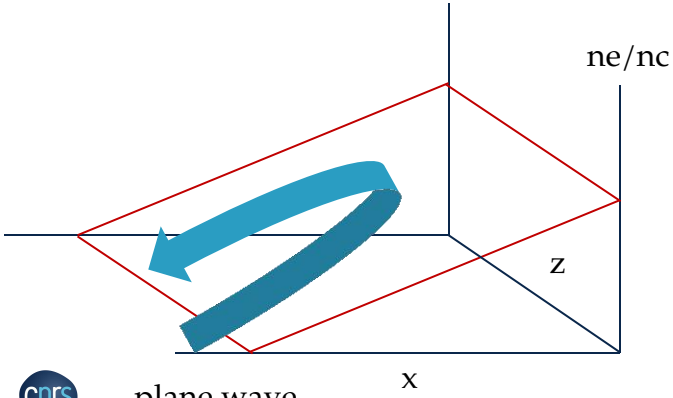

plane wave at an angle

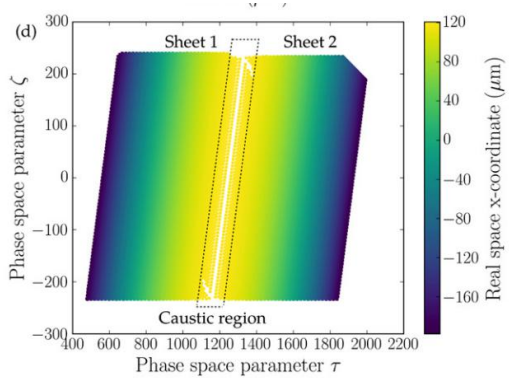

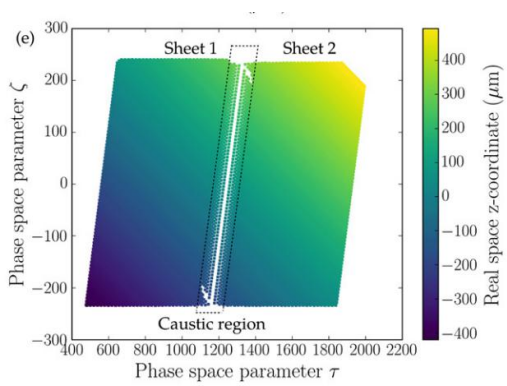

REASONABLE NUMERICAL EFFICIENCY IS OBTAINED BY LEVERAGING INVERSE RAY TRACING

$$u = A\exp[\imath k_0 \psi] \ ,$$

$$\psi''(\tau) = \int_0^\tau \epsilon''(\mathbf{r}(\hat{\tau}))\mathrm{d}\hat{\tau}/2 \ ,$$

$$A(\tau) = A(0)\left|\frac{D(0)}{D(\tau)}\right|^{1/2} \ ,$$

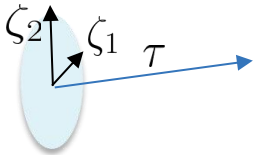

Step 1; manifold geometry
- compute the mapping from phase space (ζ_1, ζ_2) to real space (x, y)
- compute the geometric part of the laser field
- compute the Airy Integral that gives the caustic field
- compute the full Frenet frame for each sheet of each beam at each gridpoint

=> these are **geometric** factors stemming from the ray mapping
fixed during one timestep

Step 2; fields
- compute the phase contribution to the fields
- compute the Langdon effect coefficient and the polarized CBET coupling term

$$\begin{pmatrix}\epsilon_{i,j,\nu_n}\\ \epsilon_{i,j,b_n}\end{pmatrix} = [\epsilon_i' + \imath(\epsilon_{0,i}'' f_\mathrm{L} + \underline{\underline{\mathcal{D}_{i,j}}})]\cdot\begin{pmatrix}1\\1\end{pmatrix}$$

Fixed point iteration with damping until convergence

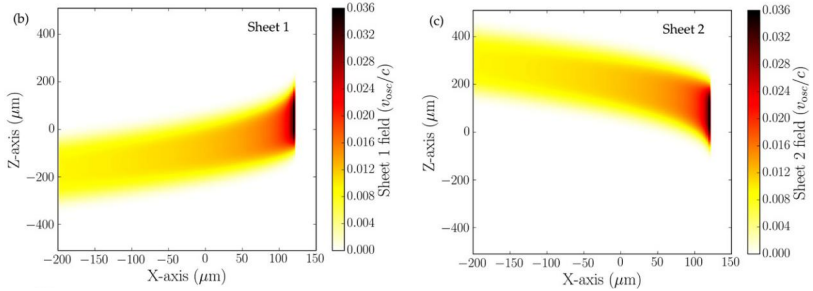

THE MODELING SYSTEMATICALLY APPROACHES THE MEASURED FLOW DIRECTION

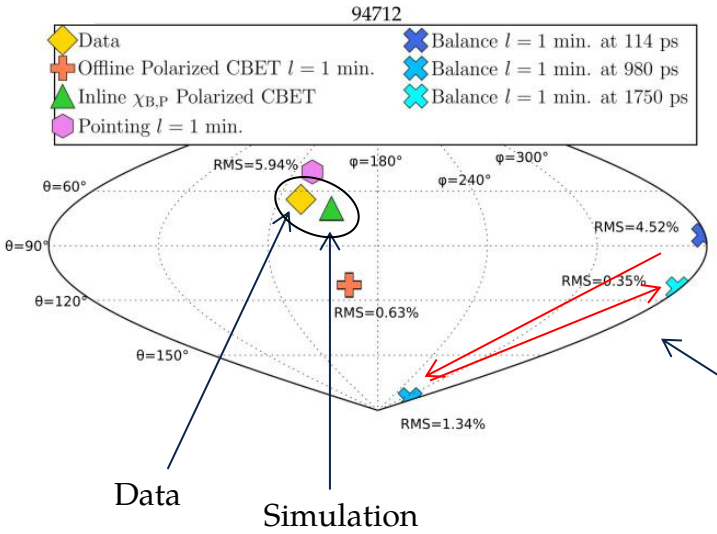

Data

Simulation

Note: the large swing in balance

94712 was dominated by pointing:
result is close to pointing anomaly

THE MODELING SYSTEMATICALLY APPROACHES THE MEASURED FLOW DIRECTION

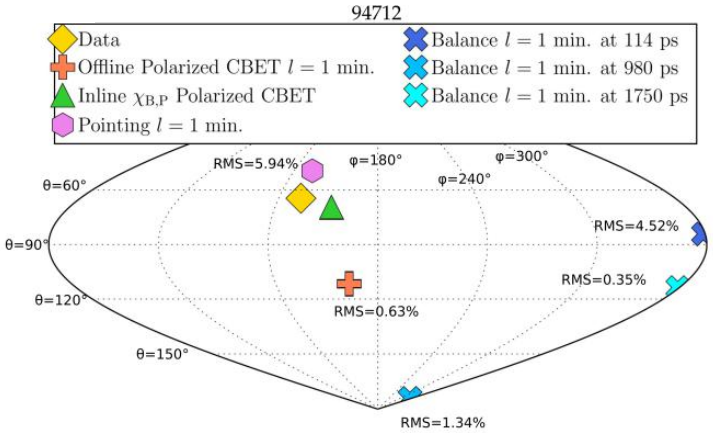

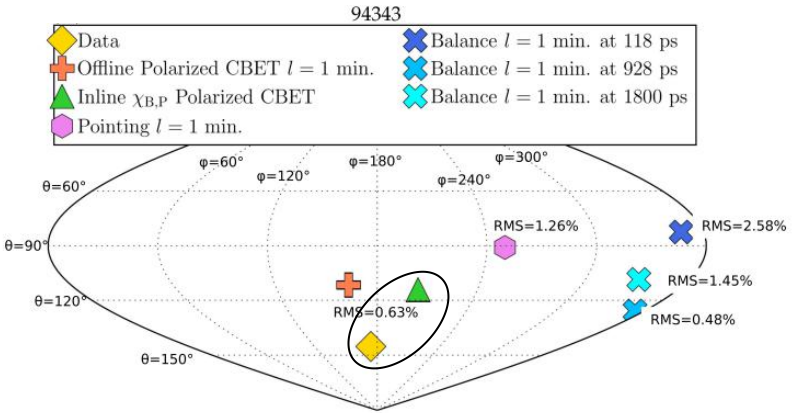

94343 had balanced low mode sources; the results is a non-trivial combination of those

THE LARGEST EFFECT ON THE DETAILS OF CBET IS THAT OF BEAM-BY-BEAM CALCULATION VS UNPOLARIZED QUADS

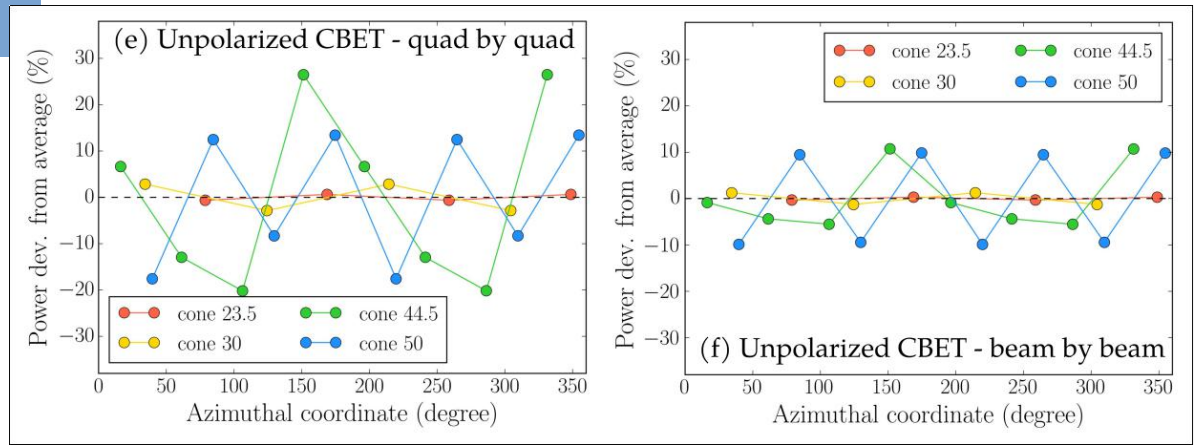

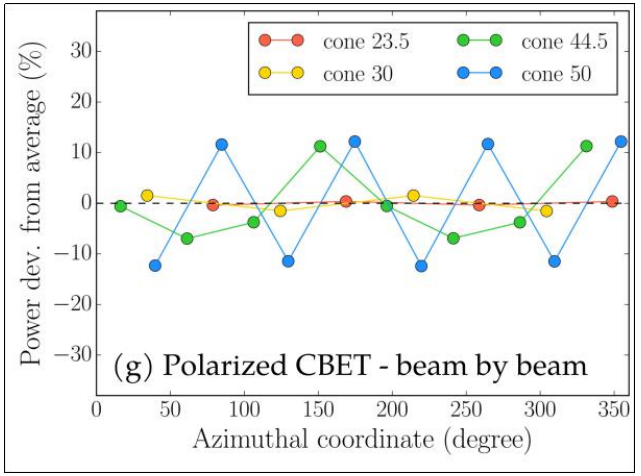

- Cone-wise, their is little effect of polarization
- In more details; polarization effect leads to more energy transfer to outer beams in cone 30 and less to outer beams in cone 44.5
- Computing the CBET beam by beam instead of quad by quad leads to less azimuthal variability in power amplification (polarized or unpolarized)